Quaternary Science Reviews 177 (2017) 57–77

Contents lists available at ScienceDirect

Quaternary Science Reviews

journal homepage: www.elsevier.com/locate/quascirev

Late-glacial and Holocene records of fire and vegetation from Cradle Mountain National Park, Tasmania, Australia

Laura N. Stahle [a, *], Hahjung Chin [b], Simon Haberle [b], Cathy Whitlock [a, c]

[a] Department of Earth Sciences, Montana State University, Bozeman, MT, USA
[b] Department of Archaeology and Natural History, School of Culture, History and Language, The Australian National University, Acton, ACT, Australia
[c] Montana Institute on Ecosystems, Montana State University, Bozeman, MT, USA

ARTICLE INFO

Article history:
Received 13 July 2017
Received in revised form
26 September 2017
Accepted 26 September 2017
Available online 5 November 2017

Keywords:
Fire history
Vegetation history
Pyrogeography
Tasmania
Fire ecology
Vegetation heterogeneity
Disturbance
Biodiversity
Vegetation dynamics

ABSTRACT

Fire activity was reconstructed at five sites and vegetation history at three sites in northwest Tasmania, Australia in order to examine the climate and human drivers of environmental change in the region. Watershed-scale reconstructions of fire were compared to regional vegetation history. Fire activity was very low until ca. 12,000 cal yr BP. An early-Holocene fire maximum, ca. 11,800–9800 cal yr BP, occurred during the warmest interval of the Holocene as recorded by regional paleoclimate proxy records. This period of elevated burning was also coincident with an increase in arboreal sclerophyll plant taxa. A maximum in rainforest taxa occurred at ca. 8500-5800 cal yr BP concurrent with sharply diminished biomass burning compared with the early Holocene. The increase in rainforest taxa is attributed to elevated effective moisture during this period. Conditions were drier and variable in the late Holocene as compared with earlier periods. A rise in fire activity at ca. 4800-3200 cal yr BP was accompanied by an increase in sclerophyll taxa and decline of rainforest and subalpine taxa. Elevated palynological richness during the late Holocene co-occurred with high levels of charcoal suggesting that fires promoted high floristic diversity. At Cradle Mountain, there is no clear evidence that fire regimes or vegetation were extensively modified by humans prior to European settlement. Climate was the primary driver of fire activity over millennial timescales as explained by the close relationship between charcoal and climate proxy data.

1. Introduction

Understanding the long-term roles of climate and people on fire and vegetation in Tasmania has been an active area of investigation for decades. Work by Macphail and Colhoun in particular were instrumental in establishing the sequence of postglacial vegetation development in western Tasmania (e.g. Colhoun and van de Geer, 1986; Colhoun et al., 1999; Macphail, 1979). Additional paleoecological studies have been published from the Central Plateau (Dodson, 2001), Lake St Clair (Hopf et al., 2000), southwest Tasmania (Fletcher and Thomas, 2007a), the Hartz Mountains (Fletcher et al., 2014a), eastern Tasmania (Mackenzie and Moss, 2014), Flinders Island (McWethy et al., 2016), and western Tasmania (Anker et al., 2001; Fletcher and Thomas, 2010b). High-resolution fire history information in Tasmania is limited to a handful of charcoal-based studies that cover the entire Holocene (Beck et al., 2017; Fletcher et al., 2015; Mariani et al., 2017; McWethy et al., 2016; Rees et al., 2015; Stahle et al., 2016), and two that span the mid-Holocene to present (Fletcher et al., 2014a,b). Many of these studies highlight the ecological importance of climate variations on centennial to millennial timescales, most notably the effects of a cool late-glacial period, warm dry early Holocene, wet mid-Holocene, and highly variable late Holocene.

People entered Tasmania at least 40,000 years ago (Cosgrove, 1999). Little is known about how Aboriginal peoples may have used fire in the Pleistocene and much of the Holocene and the questions of whether, how, and when Aboriginal Tasmanians may have altered the landscapes through their use of fire is still unclear (e.g. Bowman et al., 2013; Bowman, 1998; Ellis, 1985; Fletcher and Thomas, 2010a; Gammage, 2008, 2011; Gott, 2002, 2005; Holz et al., 2015; Hope, 1999; Jackson, 1968, 1999; Jones, 1969; Mariani et al., 2017; McIntosh et al., 2009; McWethy et al., 2016; Onfray, 2012; Romanin et al., 2016; Stahle et al., 2016; Thomas, 1993). Anthropological research, the accounts of European colonizers, and

* Corresponding author.
E-mail address: laura.stahle@msu.montana.edu (L.N. Stahle).

https://doi.org/10.1016/j.quascirev.2017.09.010
0277-3791/

landscape structure analysis suggest that Aboriginal peoples actively managed parts of the Tasmanian landscape through their use of fire to facilitate hunting and travel (Bowman, 1998; Gammage, 2008, 2011; Gott, 2005; Marsden-Smedley and Kirkpatrick, 2000; Onfray, 2012). It is believed that the primary uses of anthropogenic fire were to enhance hunting success and facilitate travel (Jackson, 1968, 1999; Bowman, 1998; Cosgrove et al., 1990; Gammage, 2008, 2011; Gott, 2005). In particular, fire was used to create patches of open land interspersed with woodlands. Grassland patches would have attracted favored prey species, especially wallabies, while the woodland patches served as areas where hunters could move relatively undetected (Gammage, 2008, 2011). The goal of Aboriginal fire management is thought to have been to make hunting more predictable (Gammage, 2008, 2011). The burning strategy consisted of low-intensity fires usually set in wetter seasons or after a rainfall event (Marsden-Smedley and Kirkpatrick, 2000). A longstanding issue in Tasmanian ecology concerns whether or not deliberate burning substantially influenced the natural fire regimes and vegetation.

In this paper, we describe the postglacial fire and vegetation in the northern sector of Cradle Mountain-Lake St Clair National Park based on pollen and charcoal records from small lakes in close proximity. This multi-site study lies in a small but heterogeneous area that enables us to investigate the spatio-temporal dynamics of fire and vegetation. The objectives of this paper are to: 1) reconstruct the postglacial vegetation and fire history of the Cradle Mountain based on new paleoecological records; and 2) compare the reconstruction with paleoenvironmental and archeological data from the region to disentangle the role of climate and people in shaping the vegetation and fire history. We hypothesize that climate was the primary driver of changes in vegetation and fire activity with anthropogenic burning playing a secondary role. We further hypothesize that climate-driven changes in the vegetation mosaic through time explain shifts in the intensity and pattern of land use.

2. Study area

Cradle Mountain-Lake St Clair National Park (CM-LSCNP) is located in northwest Tasmania, Australia and is part of the Tasmanian Wilderness World Heritage Area, a UNESCO World Heritage Area. Hereafter, we refer to our study area as Cradle Mountain. The study lakes, Lake Hanson (41.663°S 145.973°E; 1007 m), Lake Lilla (41.652°S; 145.955°E; 933 m), Lake Wilks (41.673°S 145.955°E; 1060 m), Suttons Tarn (41.683°S 145.934°E; 1099 m), and Wombat Pool (41.650°S 145.950°E; 998 m), are located in the northern sector of the national park (Fig. 1; Table 1). The lakes are located within 0.6–5.0 km of each other in a topographically complex landscape scoured by late Pleistocene glaciation (Colhoun, 1980; Thrush, 2008). Dolerite, quartzite, and basalt underlie the study area. Soils are nutrient poor on dolerite and quartzite substrates while basalt-derived soils are more nutrient-rich and fertile.

The national park is located in the transition zone between eastern Tasmania, which has a drier climate and more fertile soils, and the western half of the state, which receives more precipitation and generally has infertile soils. Precipitation in Cradle Mountain is associated with the strength and latitudinal position of the Southern Hemisphere Westerly Winds (SWW), which influences the position of storm tracks. As a result of north-to-south mountain ranges, a strong west-to-east precipitation gradient exists on the island and the western mountains receive substantial orographic rainfall. At Cradle Mountain, the annual precipitation is 2650 mm with one-third falling in winter (JJA; Waldheim station at Cradle Valley, 903 m; Bureau of Meteorology; http://www.bom.gov.au/climate/averages/tables/cw_096005.shtml; Fig. 1C). From 1917 to 2009, average winter (JJA) minimum temperature was −0.3 °C and average summer (DJF) maximum temperature was 16.3 °C. Precipitation anomalies are associated with the Southern Annular Mode (SAM) and El Niño/Southern Oscillation (ENSO). In western Tasmania, a positive SAM phase is associated with reductions in winter rainfall, whereas a negative SAM is associated with increases in rainfall in spring and summer (Hendon et al., 2007). In northern Tasmania, ENSO explains between 10 and 40% of rainfall variability and the relationship is strongest in winter (Risbey et al., 2009). During El Niño years, conditions are anomalously dry in Cradle Mountain while during La Niña years rainfall is above average (Hill et al., 2009). A strong relationship exists in Tasmania between annual area burned and October–May (i.e. spring, summer and fall) rainfall (Nicholls and Lucas, 2007; Williamson et al., 2016).

Present-day vegetation in Cradle Mountain is composed of a diverse mosaic of vegetation types including temperate rainforest, wet sclerophyll forest, woodland and shrub communities, mixed forest containing rainforest and *Eucalyptus* species, areas of moorland dominated by buttongrass (*Gymnoschoenus sphaerocephalus*), small grassland patches, and alpine shrublands and herblands (Kirkpatrick and Balmer, 1991). Many endemic plants occur in the area, including the conifer species *Athrotaxis selaginoides* and *A. cupressoides*. These culturally and ecologically important conifer trees grow in temperate rainforest and subalpine forest stands. Key rainforest trees include the two *Athrotaxis* species, *Nothofagus gunnii* (synonym = *Fuscospora gunnii*), *N. cunninghammii* (synonym = *Lophozonia cunninghammii*), and *Phyllocladus aspleniifolius*. For consistency with fossil records, *Nothofagus* will be used in place of the newer genus names (Hill et al., 2015). Many types of cool temperate rainforest persist in Cradle Mountain including *Athrotaxis-N. gunnii* short rainforest, *A. cupressoides* open woodland, *N. gunnii* rainforest and scrub, *A. selaginoides* rainforest, *A. cupressoides* rainforest, *A. selaginoides* subalpine scrub, and *Nothofagus-Atherosperma* rainforest (Harris and Kitchener, 2005).

The vegetation consists of both pyrophobic and pyrophytic plant communities. All temperate rainforests are classified as "extremely fire sensitive" indicating the ecological impact from a single fire is potentially high (Pyrke and Marsden-Smedley, 2005). Similarly, the rainforest-related alpine shrub species *Podocarpus lawrencii*, *Microcachrys tetragona*, *Diselma archeri*, and *Microstrobus niphophilus* (Kirkpatrick and Bridle, 2013) are extremely fire sensitive (Pyrke and Marsden-Smedley, 2005). Subalpine Eucalypts are also an important component of the vegetation mosaic in Cradle Mountain. *Eucalyptus subcrenulata* and *E. coccifera* co-occur in subalpine, sclerophyll woodland and open scrub communities (Wells and Hickey, 2005). These communities are classified as having "high fire sensitivity" which indicates they are fire-adapted communities that require at least 30 years between fires to maintain the defining species, while fire intervals greater than 80 years are required to reach mature stand structure (Pyrke and Marsden-Smedley, 2005). Shrubland and swamp forest plants from the Proteaceae, Myrtaceae, Ericaceae and other families are found in wet sclerophyll forest and scrub, mixed forest and moorland locales. These communities, except buttongrass moorlands, are classified as moderately fire sensitive indicating they are fire-adapted communities requiring at least 15 years between fires to maintain the dominant species (Pyrke and Marsden-Smedley, 2005). Buttongrass moorlands with and without emergent shrubs are considered to have low fire sensitivity indicating these communities are highly fire-adapted and that fire generally does not affect biodiversity (Pyrke and Marsden-Smedley, 2005).

The study lakes are presently occupied by a mosaic of the different vegetation communities that exist in Cradle Mountain.

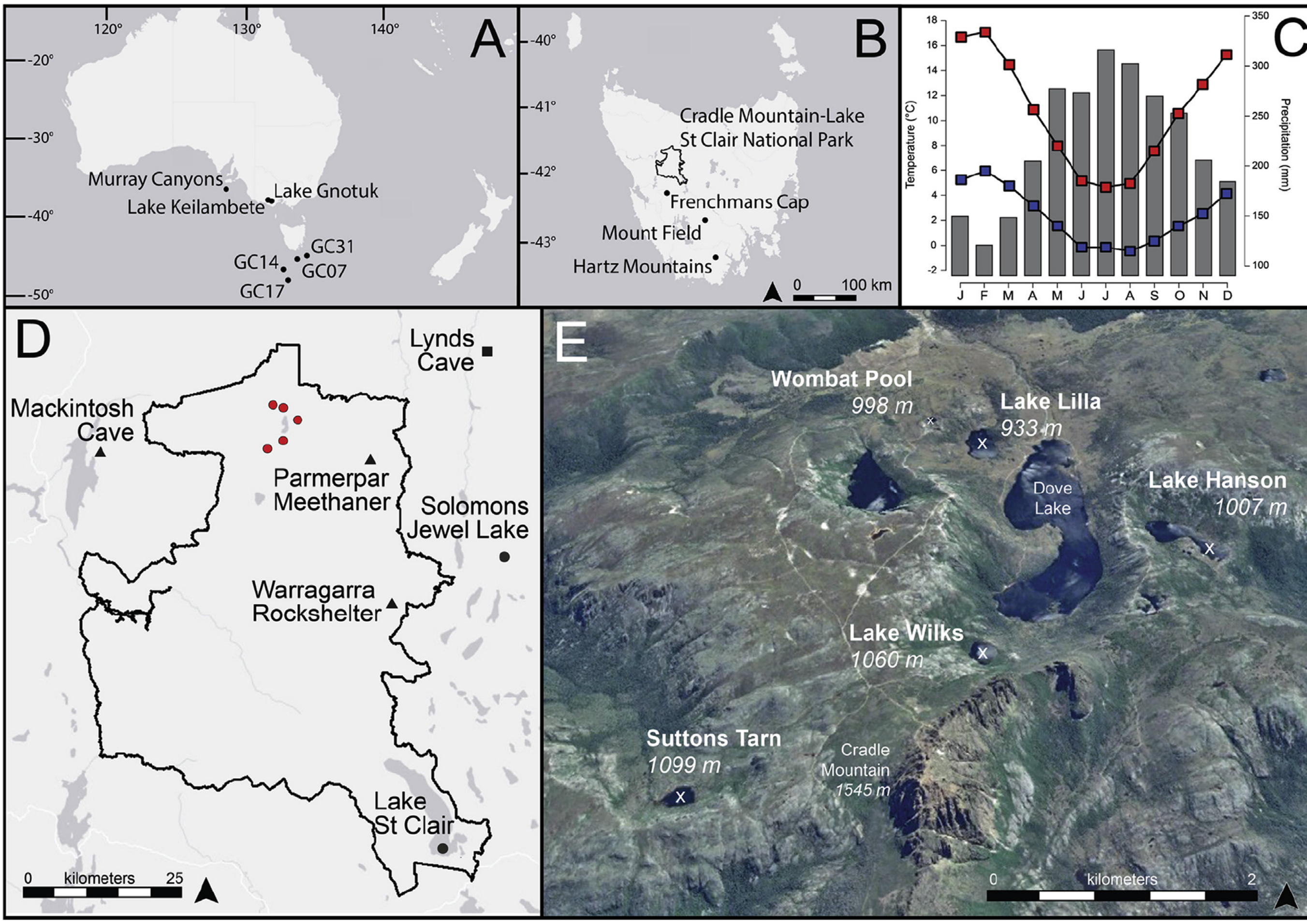

Fig. 1. Location and modern climate of study area. (A) Map of Australia with location of regional climate data (black circles = marine and lake sediment records) discussed in the text. (B) Map of Tasmania with Cradle Mountain-Lake St Clair National Park (black line) and other paleoecological sites discussed in the text (black circles). (C) Monthly climate data for Cradle Mountain-Waldheim Station (#096995; 41.64° S, 145.94° E, 903 m a.s.l.). Mean maximum temperature (red) and mean minimum temperature (blue;°C) 1926–1977, and mean precipitation (gray bars; mm) 1917–2009. (D) Map of Cradle Mountain-Lake St Clair National Park with location of study lakes (red circles), archeological sites (triangles), speleothem record (black square), and other lake records discussed in the text (black circles). (E) Satellite image of study area with study lakes (white Xs), Dove Lake, and Cradle Mountain. (For interpretation of the references to colour in this figure legend, the reader is referred to the web version of this article.)

Table 1
Site & core information.

Site	Position	Elevation (m a.s.l.)	Surface Area (ha)	Record Length (cm)	Water Depth (m)	Publication
Lake Hanson	41.663°S 145.973°E	1007	8.4	135.0	6.5	This manuscript
Lake Lilla	41.652°S; 145.955°E	933	7.2	81.5	13.2	This manuscript
Lake Wilks	41.673°S 145.955°E	1060	2.7	277.0		This manuscript
Suttons Tarn	41.683°S 145.934°E	1099	2.0	115.0	10.5	This manuscript
Wombat Pool	41.650°S 145.950°E	998	0.4	331.0	2.0	Stahle et al., 2016

Lake Hanson is surrounded by a mature cool, temperate rainforest, areas of mixed forest, and *N. gunnii* stands. Lake Lilla is surrounded by wet sclerophyll forest and shrub, buttongrass moorland, and mixed forest containing rainforest trees (*N. cunninghammii*, *A. selaginoides*, *Phyllocladus aspleniifolius*) and *Eucalyptus* species. The Lake Wilks basin is occupied by *Athrotaxis* rainforest, substantial patches of *N. gunnii*, *Eucalyptus* woodland, and coniferous alpine heathland. Suttons Tarn watershed supports a mix of *N. gunnii*-dominant cool, temperate rainforest and coniferous alpine heath. Finally, Wombat Pool is surrounded by a mosaic of wet sclerophyll forest and shrub communities, areas of buttongrass, mixed forest, and alpine shrubland. *A. cupressoides* of different age classes grows directly on the edge of all study lakes.

3. Material and methods

3.1. Field

Sediment cores were obtained from five small lakes in 2012 and 2013 from an anchored platform in the deepest water (Table 1). Cores from Lake Hanson, Lake Wilks, and Wombat Pool were obtained with a modified Livingstone piston sampler. A 6-cm-diameter polycarbonate tube attached to a universal gravity corer was used to collect cores from Lake Lilla and Suttons Tarn. The mud-water interface was captured with a plastic piston corer at Lake Hanson, Lake Wilks, and Wombat Pool. Cores from Lake Hanson, Lake Wilks, and Wombat Pool were extruded in the field and wrapped in cellophane and aluminum foil, while the entire cores were kept intact from Lake Lilla, and Suttons Tarn. The Lake Wilks samples were transported to the Australian National University, and cores from the other five sites were shipped to the National Lacustrine Core Facility (LacCore) at the University of Minnesota for initial lithological analyses.

3.2. Chronology and lithology

Bulk sediment samples were submitted for radiocarbon dating from each lake. Radiocarbon ages were calibrated using the Southern Hemisphere radiocarbon calibration dataset SHCal13 (Hogg et al., 2013). Chronologies were developed by modeling sediment age as a function of sediment depth using Clam v2.2 (Blaauw, 2010). The published chronology for Wombat Pool (Stahle et al., 2016) was used.

Core description, imaging, and magnetic susceptibility measurements for L. Hanson, L. Lilla, and Suttons Tarn were performed at LacCore. Cores were split lengthwise and one half was reserved as the archival half and the other working half was later destructively sampled. The archival halves of the cores from these three sites are stored at the Paleoecology Laboratory at Montana State University. For L. Hanson, L. Lilla, and Suttons Tarn, magnetic susceptibility (MS), which measures changes in inorganic allochthonous sediment input from erosional processes (Gedye et al., 2000), was measured at 0.5-cm continuous intervals.

3.3. Pollen analysis

Pollen analysis was undertaken on the Lake Hanson and Suttons Tarn cores. Samples of 0.25–1.0 cm^3 volume were taken at 0.25–10.0 cm core-depth intervals and prepared using methods described in Bennett and Willis (2001). Pollen grains were identified at 400x and 1000x magnification to the lowest taxonomic level possible, and terrestrial pollen counts exceeded 300 grains per sample. Identifications were based on the Australasian Pollen and Spore Atlas (apsa.anu.edu.au; APSA-Members, 2007), the pollen reference collection at the Australian National University, and the online Newcastle Pollen Collection (Hopf et al., 2005). Pollen percentages were based on the terrestrial sum (trees, shrubs, herbs, and terrestrial pteridophytes). The pollen diagrams were grouped according to modern affinities: 'Rainforest and Subalpine taxa', 'Sclerophyll Woodland taxa', 'Grassland and Herbland taxa', and 'Wetland taxa'. A *Lycopodium* tracer was added to the pollen samples to calculate pollen concentration and pollen influx.

Interpretation of the pollen percentage data was based on a comparison with modern pollen data from Cradle Mountain lake-sediment samples and with the extensive dataset published by Fletcher and Thomas (2007b). Interpretation of modern pollen data is subject to issues of representation due to variations in pollen production and dispersal among plants. The descriptions of our pollen diagrams are presented in light of the work of Fletcher and Thomas (2007b) which characterized the pollen types of western Tasmania by their dispersal ability and fidelity (Table 3). The pollen-percentage record was divided into zones by visual inspection and constrained cluster analysis (CONISS; Grimm, 1988). Pollen diagram plots and CONISS analysis were made using the program Tilia v2.0 (Grimm, 1990).

Generalized Additive Models (GAMs) were used to construct composite records of vegetation (i.e. rainforest taxa, sclerophyll taxa, subalpine taxa, wetland taxa, grassland taxa) and palynological richness following the method described by Iglesias and Whitlock (2014). We estimated temporal trends in palynological richness in order to explore changes in biodiversity through time. Palynological richness is defined as the number of terrestrial pollen and spore types present in a pollen assemblage using a constant pollen sum value (Birks and Line, 1992). Palynological richness was calculated using Psimpoll version 4.27 (Bennett, 2009) for Lake Hanson, Suttons Tarn and Wombat Pool using rarefaction to 317, 313, and 340 grains, respectively, as these were the minimum pollen counts for any sample in the three sequences. We also examined palynological evenness, or equitability of pollen types in each sample, in order to assess whether palynological richness was unduly influenced by the changes in taxonomic variability. Evenness was calculated as the inverse slope of the rank-order abundance of taxa exceeding 0.3% in each sample following Giesecke et al. (2014) using the Vegan package (Oksanen et al., 2015) in the R programming language v3.2.2 (R Core Team, 2015) using the script developed by Giesecke et al. (2014). Finally, square chord distance (SCD) was used to assess the differences between the pollen taxa assemblages (Gavin et al., 2003) and calculated using the R package analogue v0.16-3 (Simpson, 2007; Simpson and Oksanen, 2015). For L. Hanson, Suttons Tarn, and Wombat Pool, the pollen sample with the highest ratio of rainforest and subalpine taxa (65.0 cm, 57.5 cm, and 42.0 cm, respectively) to sclerophyll taxa was used as the baseline for comparison in order to identify how different the pollen assemblage in each sample was to a temperate rainforest assemblage (Macphail, 1975; Fletcher and Thomas, 2007b). A regime shift index (RSI) algorithm (Rodionov, 2004) was then applied to the SCD time series (Huber's WF = 5, $P > 0.1$, cut-off = 10 samples) in order to identify regime shifts in vegetation assemblages.

3.4. Charcoal analysis

Charcoal analysis was performed on 2-cm^3 volume samples taken at continuous 0.5-cm intervals at four sites and 1.0-cm intervals at Lake Wilks following the method described by Whitlock and Larsen (2001). Samples were washed through a 125-μm mesh sieve, and charcoal particles from the residues were counted under a stereomicroscope at 40x magnification. Charcoal particles in this size fraction (i.e. macroscopic charcoal) are deposited relatively close to their source area and widely used as a proxy of local fire activity (Clark, 1988; Whitlock and Larsen, 2001). Charcoal concentrations and deposition times were calculated and converted to charcoal accumulation rates (CHAR; particles cm^{-2} yr^{-1}).

To account for temporal variations in sampling intervals resulting from variable sedimentation rates, the CHAR time series was interpolated to the median resolution of each record (Higuera et al., 2010). CHAR was then decomposed into background (BCHAR) and peak components (Higuera et al., 2009; http://CharAnalysis.googlepages.com) with a 1250-yr lowess smoother robust to outliers. A mixed Gaussian model was used to decompose the high frequency component of the time series into "noise" and "peaks," the peak component being the 95th percentile of the noise population (Higuera et al., 2009). Charcoal peaks are assumed to represent one or more fires during the time span of the peak (referred to as "fire episodes"). Peaks were tested for statistical significance by comparing the original charcoal counts with the values of the previous five samples. Where the peak count had at least a 0.5% chance of coming from the same Poisson-distributed population as the smallest number of charcoal particles counted in the preceding five samples, the peak was considered insignificant (Higuera et al., 2009). The suitability of the records for fire-episode identification was assessed with a signal-to-noise index (SNI; Kelly et al., 2011), and only periods where SNI > 3.0 were considered appropriate for charcoal-peak interpretation. A 1000-yr bandwidth was used to calculate the SNI. Fire size and/or intensity were inferred from the magnitude of charcoal particle counts for individual peaks (Higuera et al., 2009).

The fire history was divided into Fire Intervals (FI) applying the regime-shift index (RSI) algorithm described by Rodionov (2004) to the CHAR time series. It incorporated a sequential Student's *t*-test (Huber's WF = 5, $P > 0.01$, cut-off = 20 samples) and determined where significant changes in the mean values of two adjacent regimes occur. These transitions were used to delineate fire-regime intervals. Plots were made in R v3.2.2 (R Core Team, 2015). As with the vegetation types, Generalized Additive Models (GAMs) were used to construct composite records of charcoal following the method described by Iglesias and Whitlock (2014).

4. Results

4.1. Chronology and lithology

A total of 32 radiocarbon samples from four cores (L. Hanson = 8, L. Lilla = 8, L. Wilks = 10, Suttons Tarn = 6) were submitted to Woods Hole NOSAMS AMS facility and for radiocarbon dating analysis (Table 2). Preliminary models for the four sites were developed by independently modeling age as a function of depth in each core. The final age-depth models were developed by Monte Carlo fitting smoothing splines through the probability distribution of all calibrated ages in Clam v2.2 (Blaauw, 2010, Fig. 2). The same degree of smoothing (0.4) was used in the construction of all four chronologies. The published age-depth model for Wombat Pool was used (Stahle et al., 2016).

The core lithology for L. Hanson, L. Lilla, and Suttons Tarn is displayed in Fig. 3. Each record contained two units. These units were determined by visual analysis and magnetic susceptibility.

L. Hanson Unit 1 (135.0–129.5 cm depth; 13,030–12,715 cal yr BP) consisted primarily of inorganic silt and clay. Magnetic susceptibility was high in this period (−1.3 to −0.1 SI units; mean = −1.355) indicating substantial mineral clastic input (Gedye et al., 2000). L. Hanson Unit 2 (129.5–12.5 cm depth; 12,715–1586 cal yr BP) was composed of fine-detritus gyttja. Magnetic susceptibility was generally lower in this period (−2.1 to 1.4 SI units; mean = −0.607) suggesting more organic sediment than Unit 1. Unit 2 included an increase in MS between 35.0 and 33.0 cm depth (4705–4429 cal yr BP), which was associated with a change in lithology toward clay-rich sediments and contemporaneous with a fire event. This interval is the only depth where fire and MS had concurrent increases.

L. Lilla Unit 1 (83.0–68.5 cm depth; 15,175–12,735 cal yr BP) contained inorganic clay and silt with high MS values (0.4 to −0.8 SI units; mean = −0.272). Unit 2 (68.5–12.5 cm depth; 12,735–2550 cal yr BP) was composed of fine-detritus gyttja and had lower MS values (−0.4 to −1.6 SI units; mean = −1.094).

Suttons Tarn Unit 1 (116.0–109.0 cm depth; 16,600–16,000 cal yr BP), like the basal units in the other cores, was mostly inorganic clay and silt with elevated MS values (1.8–1.3 SI units; mean = 1.653). Unit 2 (109.0–0.0 cm depth; 16,000– −62 cal yr BP) was primarily composed of fine-detritus gyttja with low MS values (2.6 to −1.2 SI units; mean = 0.087).

4.2. Pollen

4.2.1. Lake Hanson (Fig. 4)

Pollen Zone 1 (HAN-1; 133.0–105.5 cm depth; 13,000–11,500 cal yr BP) was dominated by *Phyllocladus* (11–27%) and featured moderate percentages of Asteraceae and Poaceae (9% and 10%). *Pomaderris* values were between 6 and 9%. *Eucalyptus* fluctuated between 6 and 13%. Woody sclerophyll taxa including *Leptospermum-Baeckea*, Proteaceae, and Ericaceae were at moderate amounts in this zone (2%, 2% and 5%). Above 114.5 cm depth, *N. gunnii* increased to 12%. The pollen assemblage of this zone suggests the vegetation was moderately open with herbaceous taxa and some shrubs and trees. *Eucalyptus* and the pioneer rainforest species *Phyllocladus* were present in the region, but not likely growing locally for most of this period (Table 3; Fletcher and Thomas, 2007b).

Pollen Zone 2 (HAN-2; 105.5–83.0 cm depth; 11,500–9700 cal yr BP) featured high amounts of *N. gunnii* (11–18%) and sharply reduced amounts of *Phyllocladus* (2–4%). Rainforest trees increased in abundance and included *Athrotaxis* (4–5%), *Anodopetalum-Eucryphia* (4–5%), and *N. cunninghammii* (32–38%). *Pomaderris* and *Eucalyptus* remained at moderate values in this period (7–10% and 8–12%) and *Leptospermum-Baeckea* and Ericaceae were present in small amounts (2–4%). Poaceae and Asteraceae declined (2–5% and 1–3%). This pollen assemblage suggests that the vegetation resembled a modern *N. gunnii* rainforest with substantial scrub rainforest elements (Harris and Kitchener, 2005).

Pollen Zone 3 (HAN-3; 83.0–31.0 cm depth; 9700–4250 cal yr BP) featured the highest amounts of *N. cunninghammii* in the record. At 81.0 cm depth (ca. 9550 cal yr BP), values reached >40% indicating a local presence (Fletcher and Thomas, 2007b). During this zone, *N. cunninghammii* fluctuated between 35 and 47% (mean = 41%) and peaked at 53.0 cm depth (ca. 6900 cal yr BP). *Athrotaxis-Diselma* type also achieved its highest values of the record in this zone (8%) at 62.0 cm depth (ca. 7800 cal yr BP) while oscillating between 3 and 9% (mean = 5%). *N. gunnii* values were lower than Zone 2 but retained moderate amounts in Zone 3 (6–12%, mean = 9%). Other rainforest taxa, including *Anodopetalum-Eucryphia* (2–8%), *Phyllocladus* (7–12%), *Pomaderris* (4–8%), and *Dicksonia antarctica* (up to 4%) had moderate values in this zone, especially after 69.0 cm depth (ca. 8500 cal yr BP). The local vegetation in this period was similar to a modern temperate rainforest dominated by *N. cunninghammii* (Harris and Kitchener, 2005).

Pollen Zone 4 (HAN-4; 31.0–0.0 cm depth; 4250 to −61 cal yr BP) featured an increase in wet sclerophyll woodland taxa and a reduction in rainforest and subalpine taxa. *Eucalyptus* reached the highest values of the record (21%) and maintained amounts between 14 and 21% (mean = 16%) from 29.0 to 2.0 cm depth (ca. 4000-200 cal yr BP). Ericaceae maintain moderate amounts (2–8%, mean = 4%) during this zone and the taxon also achieved its maximum in this period (8%). Other wet sclerophyll woodland taxa equaled or exceed their highest amounts for the record, including *Leptospermum-Baeckea* (4%), *Monotoca* (2%), and *Casuarina* (3%).

4.2.2. Suttons Tarn (Fig. 5)

Pollen Zone 1 (SUT-1; 110.5–97.5 cm depth; 16,100–15,000 cal yr BP) is dominated by grasses and forbs as evidenced by high abundances of Poaceae (up to 15%) and Asteraceae (up to 21%). *Casuarina*, Chenopodiaceae, and combined aquatic taxa had their highest values of the record in this period (9%, 5%, and 7%). This pollen assemblage indicates an open landscape of alpine herbs and forbs (Harris and Kitchener, 2005).

Pollen Zone 2 (SUT-2; 97.5–72.0 cm depth; 15,000–12,500 cal yr BP) was distinguished by high values for *Phyllocladus* (19–29%). Poaceae and Asteraceae declined from Zone 1 but remained in moderate amounts (7–9% and 8–12%). *Dichosciadium-Xanthosia* type (Apiaceae family), *Astelia alpina*, *Pomaderris*, and Proteaceae reached their highest values of the record during this period (7%, 4%, 9% and 3%). This pollen assemblage suggests a grassland-forest mosaic with a mix of herbaceous and woody subalpine elements near the lake and regional coverage of the pioneer rainforest species *Phyllocladus* (Harris and Kitchener, 2005).

Pollen Zone 3 (SUT-3; 72.0–59.0 cm depth; 12,500–11,100 cal yr BP) is marked by increases in subalpine taxa. *Athrotaxis-Diselma* is as high as 15%, while *Podocarpus lawrencei* and *Tasmannia*

Table 2
Radiocarbon dating results from Lake Hanson, Lake Lilla, Lake Wilks, and Suttons Tarn. Calibrations (cal yr BP) are based on the Southern Hemisphere calibration curve SHCal13.14C (Hogg et al., 2013).

Core	Cumulative Core Depth (Top; cm)	Lab Number (NOSAMS)	Material Dated	Radiocarbon Age (^{14}C yr BP)	Error (^{14}C yr BP	δ13C	Age (cal yr BP) & Probability [a]
Lake Hanson 12A	10.0	OS-108059	Bulk sediment	1510	25	−26.67	1306-1381; 89.7
							1390-1403; 5.3
Lake Hanson 12A	22.0	OS-108109	Bulk sediment	2450	30	−26.6	2347-2511; 75.5
							2528-2537; 0.8
							2590-2615; 4.5
							2634-2697; 14.2
Lake Hanson 12A	40.0	OS-108110	Bulk sediment	4900	25	−27.09	5486-5513; 10.8
							5523-5526; 0.6
							5580-5654; 83.5
Lake Hanson 12A	56.0	OS-108111	Bulk sediment	6190	25	−26.88	6954-7159; 95.0
Lake Hanson 12C	71.5	OS- 104112	Bulk sediment	8050	35	−26.71	8723-9009; 95.0
Lake Hanson 12A	72.0	OS-105542	Bulk sediment	7760	55	−26.82	8419-8583; 95.0
Lake Hanson 12C	99.5	OS- 104113	Bulk sediment	9740	40	−27.49	10812-10840; 1.9
							10867-10952; 16.2
							11070-11226; 76.8
Lake Hanson 12C	127.5	OS- 104114	Bulk sediment	10,600	40	−26.14	12431-12572; 66.5
							12581-12646; 28.5
Lake Lilla 12F	19.0	OS-105818	Bulk sediment	3660	50	−26.97	3730-3745; 1.2
							3768-3790; 1.8
							3825-4089; 91.9
Lake Lilla 12F	27.0	OS-105819	Bulk sediment	4810	35	−27.07	5330-5376; 11.7
							5453-5591; 83.2
Lake Lilla 12F	35.0	OS-105820	Bulk sediment	6300	35	−27.17	7022-7118; 17.4
							7152-7267; 77.5
Lake Lilla 12F	43.0	OS-105821	Bulk sediment	8400	55	−27.43	9143-9173; 2.5
							9208-9217; 0.6
							9239-9497; 91.9
Lake Lilla 12F	51.0	OS-106149	Bulk sediment	9070	40	−27.52	9950-9987; 3.0
							10,042–10,056; 0.9
							10,149–10,256; 91.0
Lake Lilla 12F	59.0	OS-106054	Bulk sediment	9680	40	−27.58	10,784–11,033; 56.5
							11,060–11,185; 38.4
Lake Lilla 12F	67.0	OS-106055	Bulk sediment	10,400	35	−26.57	12,023–12,317; 73.2
							12,322–12,403; 21.8
Lake Lilla 12F	75.0	OS-100719	Bulk sediment	12,200	55	−26.25	13,820–14,196; 95.0
Lake Wilks	23.0	OS-95795	Bulk sediment	660	25	−27.13	552-577; 23.6
							583-649; 71.3
Lake Wilks	35.0	OS-92425	Bulk sediment	1730	25	−26.72	1523-1630; 83.3
							1653-1691; 11.7
Lake Wilks	45.0	OS-95796	Bulk sediment	2260	35	−27.15	2128-2331; 95
Lake Wilks	46.0	OS-95791	Bulk sediment	1770	40	−26.24	1531-1714; 95
Lake Wilks	58.0	OS-92426	Bulk sediment	3590	25	−26.56	3705-3897; 95
Lake Wilks	99.0	S-ANU18729	Bulk sediment	3820	30	−23.08	3989-4046; 14.6
							4066-4240; 80.4
Lake Wilks	119.0	OS-95792	Bulk sediment	3570	45	−26.79	3642-3664; 2.7
							3683-3913; 92
							3918-3920; 0.2
							3955-3955; 0.1
Lake Wilks	163.0	OS-95793	Bulk sediment	5620	75	−27.83	6206-6503; 94.8
							6524-6526; 0.1
Lake Wilks	228.0	OS-95794	Bulk sediment	8150	120	−27.55	8636-9316; 92.8
							9358-9399; 2.1
Lake Wilks	273.0	S-ANU18026	Bulk sediment	10,055	45	−27.04	11,267–11,653; 89.3
							11,661–11,708; 5.7
Suttons Tarn 13A	10.0	OS-118680	Bulk sediment	2570	20	−26.78	2714-2752; 95.0
Suttons Tarn 13A	30.0	OS-118297	Bulk sediment	6080	20	−27.21	6891-6997; 95.0
Suttons Tarn 13A	50.0	OS-118298	Bulk sediment	8750	25	−27.78	9615-9616; 0.3
							9623-9888; 94.6
Suttons Tarn 13A	70.0	OS-118299	Bulk sediment	10,550	30	−27.5	12,421–12,509; 39.4
							12,511–12,617; 55.5

Table 2 (*continued*)

Core	Cumulative Core Depth (Top; cm)	Lab Number (NOSAMS)	Material Dated	Radiocarbon Age (^{14}C yr BP)	Error (^{14}C yr BP	δ13C	Age (cal yr BP) & Probability [a]
Suttons Tarn 13A	90.0	OS-118300	Bulk sediment	12,100	35	−27.36	13,809–14,103; 95.0
Suttons Tarn 13A	108.0	OS-118301	Bulk sediment	13,300	40	−25.33	15,811–16,170; 95.0

[a] Calibrated ages derived from Clam v2.2 and represent the 2-sigma error ranges.

Table 3
Pollen representation categories for key pollen taxa based on the analysis of dispersability and fidelity by Fletcher and Thomas (2007b).

Under-Represented	Well-Represented	Over-Represented
Athrotaxis	*Eucalyptus*	*Nothofagus cunninghammii*
Nothofagus gunnii	*Leptospermum*	*Phyllocladus*
Banksia	*Monotoca*	
Melaleuca	*Allocasuarina*	
Gymnoschoenus	Asteraceae	
Ericaceae	Poaceae	
Eucryphia/Anodopetalum		
Microstrobos		
Microcachrys		

lanceolata reach 4% and 3%, respectively. *N. gunnii* increases to 9% and *Phyllocladus* declines to 8% above 67.0 cm depth (ca. 12,000 cal yr BP). Asteraceae and Poaceae continued to decline (<5%). Ericaceae increased to 4–5%. The pollen assemblage in this zone suggests the presence of an *Athrotaxis-N. gunnii* short rainforest with substantial subalpine shrubs (Harris and Kitchener, 2005).

Pollen Zone 4 (SUT-4; 59.0–21.0 cm depth; 11,100–5300 cal yr BP) contained the highest values for the rainforest taxon *N. gunnii* (33–44%, mean = 38%). *Athrotaxis-Diselma* was recorded at moderate amounts (6–15%). *N. cunninghammii* was higher than in

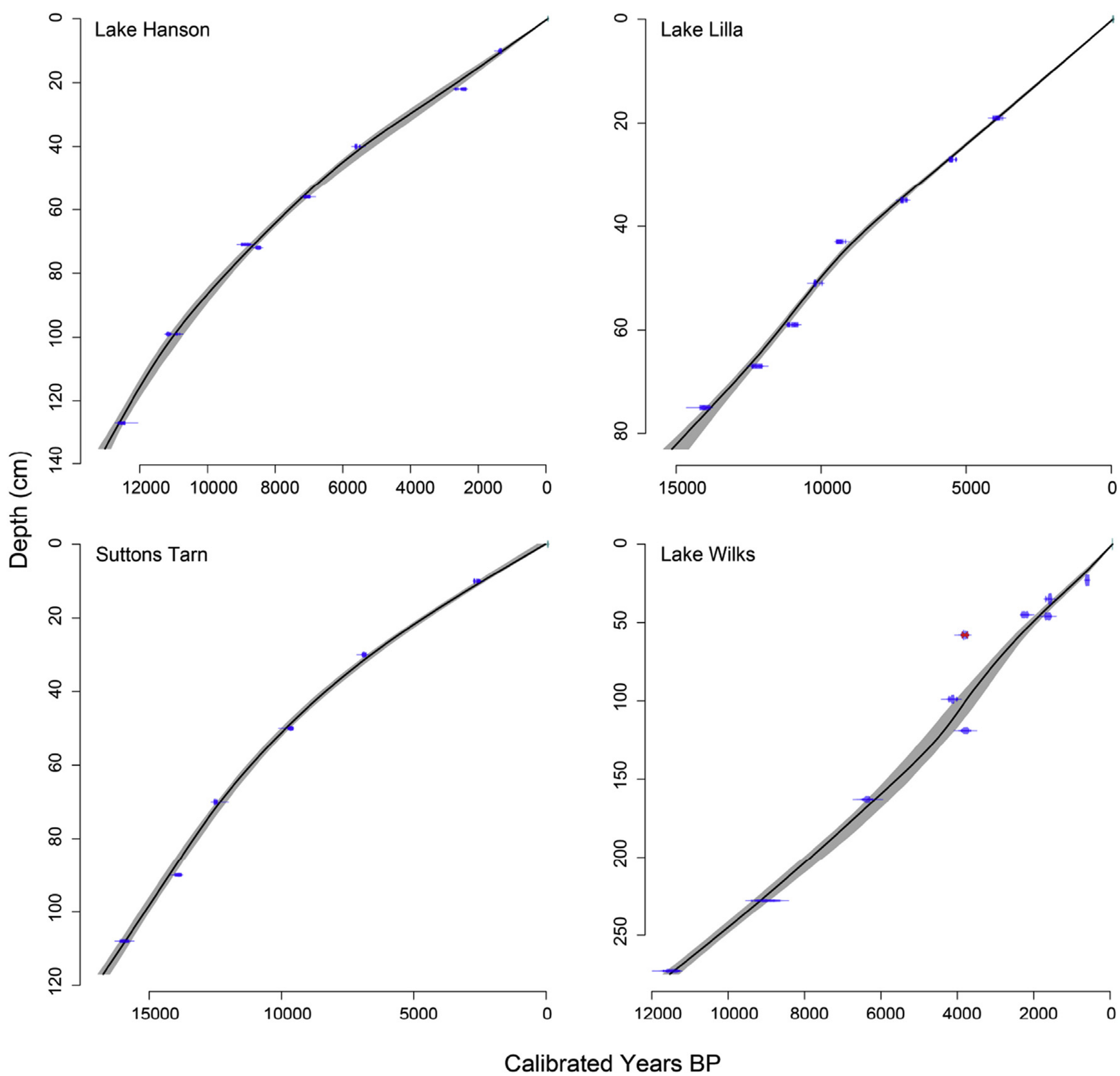

Fig. 2. Age-depth models. Age depth models (black lines) for Lake Hanson, Lake Lilla, Suttons Tarn and Lake Wilks were made using Clam v2.2 (Blaauw, 2010). The 95% confidence intervals are shown as gray shading. The distributions of the calibrated radiocarbon ages that were used to develop the models are shown in blue, and the L. Wilks date that was not included in its model is indicated in red. (For interpretation of the references to colour in this figure legend, the reader is referred to the web version of this article.)

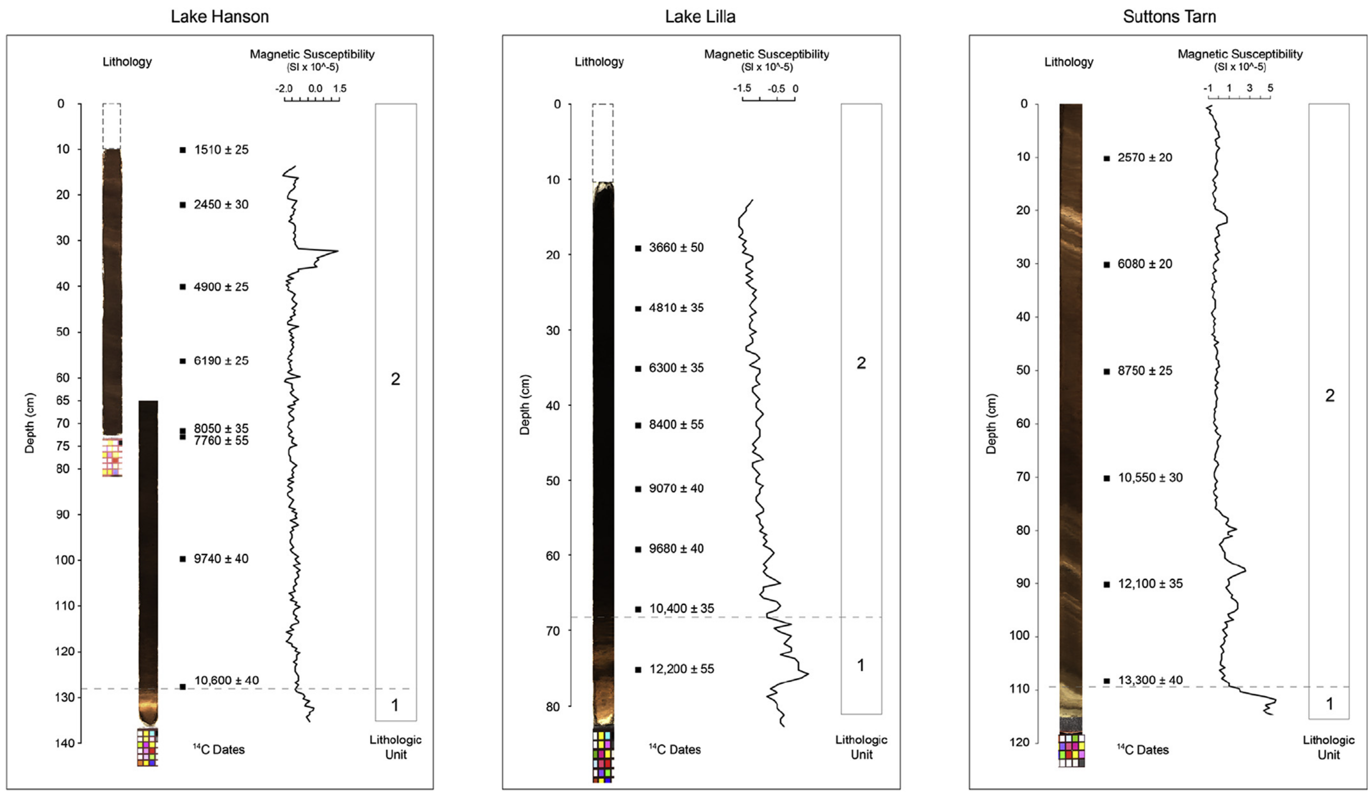

Fig. 3. Lithology. Lithology (core photographs), uncalibrated radiocarbon dates and associated errors, and magnetic susceptibility from Lake Hanson, Lake Lilla, and Suttons Tarn. The top 10 cm of the Lake Hanson and Lake Lilla records (dashed line boxes) were subsampled in the field and thus not photographed.

previous periods (23–36%), but probably too low to indicate local presence (Fletcher and Thomas, 2007b). The vegetation in this period likely resembled a modern *Athrotaxis-N. gunnii* short rainforest (Harris and Kitchener, 2005).

Pollen Zone 5 (SUT-5; 21.0–0.0 cm depth; 5300 to −62 cal yr BP) featured an increase in wet sclerophyll woodland elements and herbaceous taxa and a decline in rainforest taxa. *Eucalyptus* increased substantially during this period—up to 19% (mean = 11%). Wet sclerophyll woodland taxa also recorded increases, including *Casuarina* (up to 3%), Proteaceae (up to 2%), *Leptospermum-Baeckea* (up to 4%), and Ericaceae (4–8%). Herbaceous taxa increased as well. Asteraceae (up to 5%), Poaceae (up to 3%) and Chenopodiaceae (up to 3%) reached their highest values since the late-glacial period (i.e. Zone 2). *Athrotaxis-Diselma* and *N. gunnii* declined to 2–6% (mean = 4%) and 10–20% (mean = 14%), respectively. Rainforest shrubs increased—*Anodopetalum-Eucryphia*, *Dicksonia antarctica* and *Pomaderris* up to 4%, 3% and 6%.

4.2.3. Composite vegetation records, palynological richness, & square-chord distance

Generalized Additive Models (GAM) were employed to construct composite records of vegetation groups, as well as to composite the palynological richness curves. The two individual pollen records described above and the Wombat Pool record (Stahle et al., 2016), which represented 163 individual pollen samples, were used to build the regional composite records and estimate regional trends in vegetation. The preferred models for rainforest taxa, sclerophyll taxa, subalpine taxa, grassland taxa, and wetland taxa explained 78, 70, 73, 92, and 64% of the deviance, respectively (Fig. 9b-f; Table 4).

Palynological richness and evenness were calculated using the pollen records for L. Hanson, Suttons Tarn, and Wombat Pool (Figs. 4 and 5, Supplementary Fig. 1). The values for palynological richness varied between 19 and 29 at Lake Hanson, between 18 and 34 at Suttons Tarn, and from 15 to 29 at Wombat Pool. Evenness values were highly complacent for all three records varying at most 0.09 between samples and 0.1 over the entirety of each record out of a possible range of 0.0–1.0 (Figs. 4 and 5, Supplementary Fig. 1). The low variability in the evenness results for all three sites gave us confidence in the palynological richness results. Low variability in the evenness values means that the relative proportion of pollen types in all samples was fairly stationary indicating the richness results are robust and not unduly influenced by rare taxa (Giesecke et al., 2014). The preferred GAM for palynological richness explained 27% of the deviance (Fig. 9g; Table 4).

Square-chore distance analysis (SCD) was performed on the pollen records for Lake Hanson, Suttons Tarn, and Wombat Pool in order to understand the Holocene vegetation history of each record (Fig. 7). The SCD values for L. Hanson varied from 3.9 to 28.5, for Suttons Tarn from 6.1 to 69.9, and for Wombat Pool from 7.0 to 31.4. The lower the number for a given sample, the more similar the pollen composition of that sample is to a sample dominated by rainforest and subalpine taxa (Fletcher and Thomas, 2007b; Macphail, 1975). A regime-shift algorithm (Huber's WF = 5, $P > 0.1$, cut-off = 10 samples; Rodionov, 2004) was applied to the three SCD time series in order to identify vegetation regimes with statistically significant differences. Four regimes were identified in the L. Hanson record: 13,000–11,500 cal yr BP (mean SCD = 23.3), 11500–8150 cal yr BP (mean SCD = 11.7), 8150–4250 cal yr BP (mean = 4.6), 4250 to −61 cal yr BP (mean SCD = 12.7). Three regimes were identified in the Suttons Tarn record: 14,000–11,100 cal yr BP (mean SCD = 57.6), 11,100–4900 cal yr BP (mean SCD = 8.8), 4900 to −62 cal yr BP (mean SCD = 28.6). Finally, three regimes were identified in the Wombat Pool record:

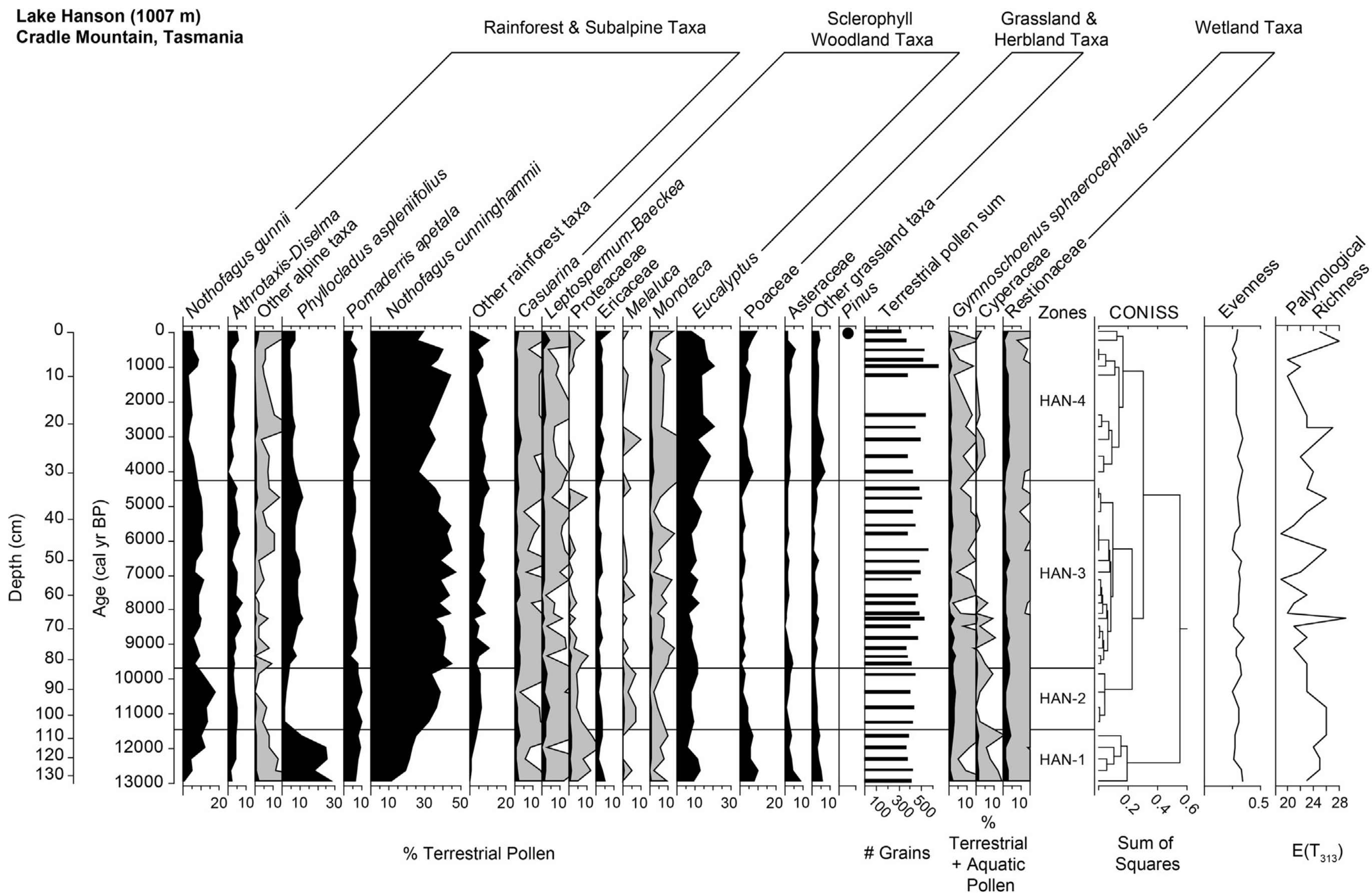

Fig. 4. Pollen diagram of selected taxa from Lake Hanson. The gray shading indicates 10x exaggeration. The uppermost sample in the record contains *Pinus* indicated by a dot. Palynological richness, and evenness data are shown at right. Palynological richness was calculated by rarefaction analysis to 317 terrestrial pollen grains as described by Birks and Line (1992) in the program psimpoll (Bennett, 2009). Evenness was calculated using the method described in Giesecke et al. (2014). Note differing scales on the x axes.

12,400–9800 cal yr BP (mean SCD = 22.6), 9800–4500 cal yr BP (mean SCD = 12.7), 4500 to −61 cal yr BP (mean SCD = 19.5). The mid-Holocene regime at each site had the lowest mean SCD values meaning that pollen assemblages were dominated by taxa of rainforest and subalpine types and the vegetation of the period included a substantial amount of cool temperate rainforest (Fletcher and Thomas, 2007b; Macphail, 1975).

4.3. Charcoal

4.3.1. Lake Hanson

The Lake Hanson charcoal record (Fig. 6) began at 13,040 cal yr BP and end at −61 cal yr BP. The median sample resolution of the record was 47 yr. CharAnalysis (Higuera et al., 2009) identified 23 fire episodes. Regime-shift analysis (Rodionov, 2004) resulted in the identification of six Fire Intervals (FI). FI 1 (134.5–131.0 cm depth, 13,020–12,850 cal yr BP) had a mean CHAR value of 0.008 particles cm^{-2} yr^{-1}. No fires were identified in this period. Fire activity was slightly elevated in FI 2 (131.0–117.0 cm depth; 12,850–12,100 cal yr BP; mean CHAR = 0.116 particles cm^{-2} yr^{-1}) and one fire was identified (2.31 particles cm^{-2} yr^{-1}). FI 3 (117.0–103.0 cm depth; 12,100–11,250 cal yr BP) was characterized by the highest biomass burning of the L. Hanson record with a mean CHAR value of 0.420 particles cm^{-2} yr^{-1}. Four fire episodes were identified (mean CHAR = 12.71 particles cm^{-2} yr^{-1}). Fire activity declined in FI 4 (103.0–77.5 cm depth; 11,250–9230 cal yr BP) but remained relatively high (mean CHAR = 0.296 particles cm^{-2} yr^{-1}). Four fire episodes were identified (two with SNI > 3.0; mean CHAR = 18.46 particles cm^{-2} yr^{-1}). Fire activity declined from FI 4 to FI 5 (77.5–64.5 cm depth; 9230–8050 cal yr BP). The mean CHAR value in FI 5 was 0.176 particles cm^{-2} yr^{-1}. Two fire episodes were recorded in this period, but the low SNI suggests that it is difficult to determine whether these were local or regional fire events (Kelly et al., 2011). The final fire interval of the record, FI 6, was very long (64.5–0.0 cm depth; 8050– −61 cal yr BP). Low CHAR characterized this period (mean CHAR = 0.064 particles cm^{-2} yr^{-1}). Twelve fire events were identified (8 with SNI > 3.0; mean CHAR = 6.410 particles cm^{-2} yr^{-1}).

4.3.2. Lake Lilla

The Lake Lilla charcoal record (Fig. 6) spaned 15,000 to −61 cal yr BP. The median resolution of the record was 89 yr. Due to the low sample resolution of this record, we employed a global threshold for peak identification rather than the more standard local thresholds in CharAnalysis (Higuera et al., 2009). Local thresholds were used for all other records. Eight fire episodes were identified in the Lake Lilla record. Regime-shift analysis (Rodionov, 2004) resulted in the identification of four Fire Intervals (FI). FI 1 (82.0–63.0 cm depth, 15,000–11,920 cal yr BP) contained virtually no charcoal (mean CHAR = 0.002 particles cm^{-2} yr^{-1}) and recorded no fires. Fire activity was elevated in FI 2 (63.0–55.5 cm depth; 11,920–10,850 cal yr BP; mean CHAR = 0.082 particles cm^{-2} yr^{-1}) and two very small magnitude fires were identified (mean peak magnitude = 1.53 particles cm^{-2} yr^{-1}). FI 3 (55.5–43.0 cm depth; 10,850–8890 cal yr BP) contained the highest biomass burning of the record (mean CHAR = 0.178 particles cm^{-2} yr^{-1}) and the largest

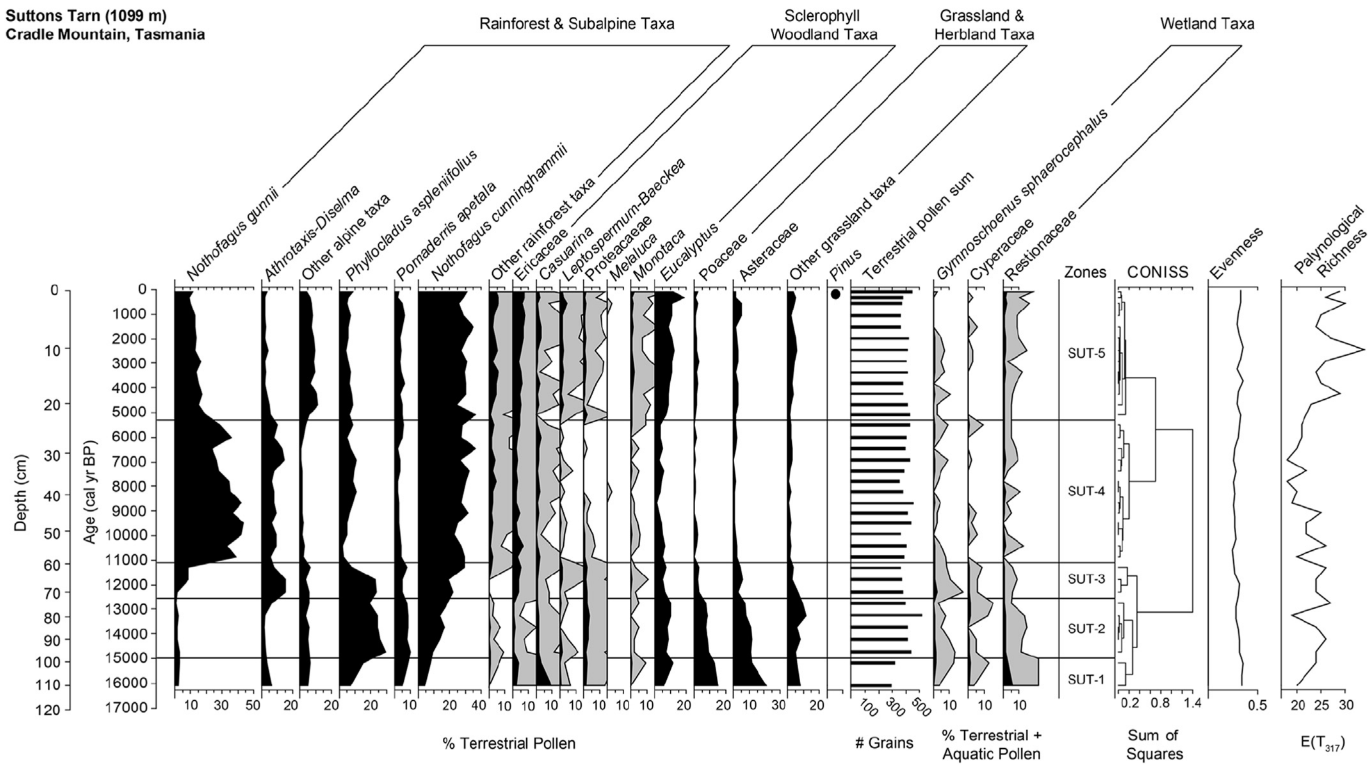

Fig. 5. Pollen diagram of selected taxa from Suttons Tarn. The gray shading indicates 10x exaggeration. The uppermost sample in the record contains *Pinus* indicated by a dot. Palynological richness, and evenness data are shown at right. Palynological richness was calculated by rarefaction analysis to 317 terrestrial pollen grains as described by Birks and Line (1992) in the program psimpoll (Bennett, 2009). Evenness was calculated using the method described in Giesecke et al. (2014). Note differing scales on the x axes.

Table 4
Models employed in the reconstruction of regional trends in vegetation, fire, and palynological richness in Cradle Mountain, and sea surface temperatures (SSTs) south of Tasmania.

Data Type	# Samples	# Sites	Smoothing (k) Parameter	Degrees of Freedom	AIC	Deviance Explained	Family	Model
Charcoal	1497	5	40	27.76	3911.99	42%	Gaussian	f(times) + site + ε_{ts}
Rainforest Pollen Taxa	163	3	15	15.87	1045.00	78%	Gaussian	f(times) + site + ε_{ts}
Sclerophyll Woodland Pollen Taxa	163	3	15	14.17	889.44	70%	Gaussian	f(times) + site + ε_{ts}
Subalpine Pollen Taxa	163	3	9	10.60	1045.86	73%	Gaussian	f(times) + site + ε_{ts}
Grassland Pollen Taxa	163	3	9	11.65	841.27	91.6%	Gaussian	f(times) + site + ε_{ts}
Wetland Pollen Taxa	163	3	10	12.23	832.77	64.4%	Gaussian	f(times) + site + ε_{ts}
Palynological Richness	163	3	10	10.27	780.28	27%	Gaussian	f(times) + ε_{ts}
Sea Surface Temperature	78	4	5	11.29	245.62	77%	Gaussian	f(times) + site + ε_{ts}

$\varepsilon \sim N(\mu,\sigma)$.

magnitude peak of the record (75.08 particles cm^{-2} yr^{-1} at 55.0 cm; 10,800 cal yr BP). Two fire events were recorded in this interval. FI 4 (43.0–0.0 cm depth; 8890– −61 cal yr BP; mean CHAR = 0.044 particles cm^{-2} yr^{-1}) was long lasting. Four fire episodes were recorded (mean peak magnitude = 7.854 particles cm^{-2} yr^{-1}), including the second largest peak of the record (28.05 particles cm^{-2} yr^{-1} at 20.5 cm; 4300 cal yr BP).

4.3.3. Lake Wilks

The Lake Wilks charcoal record (Fig. 6) began at 11,640 cal yr BP and continues to −61 cal yr BP. The median sample resolution of the record was 44 yr. Twenty-eight fires were identified by CharAnalysis (Higuera et al., 2009) and three Fire Intervals were distinguished by regime-shift analysis (Rodionov, 2004). FI 1 (277.0–121.0 cm depth; 11,640–4420 cal yr BP) had a mean CHAR value of 0.664 particles cm^{-2} yr^{-1}. Sixteen fire episodes were identified in this period (12 with SNI > 3.0; mean peak magnitude = 45.45 particles cm^{-2} yr^{-1}). FI 2 (121.0–104.0 cm depth; 4420–3900 cal yr BP) was a short interval that recorded the first and second highest magnitude fire events of the record: 361.36 particles cm^{-2} yr^{-1} (120.5 cm depth; 4400 cal yr BP) and 1203.0 particles cm^{-2} yr^{-1} (109.5 cm; 4050 cal yr BP). Mean CHAR in this period was very high (782.18 particles cm^{-2} yr^{-1}). FI 3 (104.0–0.0 cm depth; 3900– −61 cal yr BP) recorded a mean CHAR value of 0.7 particles cm^{-2} yr^{-1}. Ten fires in this period had a mean peak magnitude of 41.59 particles cm^{-2} yr^{-1}.

4.3.4. Suttons Tarn

The Suttons Tarn charcoal record (Fig. 6) spaned 16,575 to −62 cal yr BP. The median sample resolution was 64 yr. CharAnalysis (Higuera et al., 2009) identified 24 fire episodes. Regime shift analysis (Rodionov, 2004) resulted in the identification of three Fire Intervals. FI 1 (115.0–18.5 cm depth; 16,575–4320 cal yr BP) had a mean CHAR value of 0.065 particles cm^{-2} yr^{-1}, and 19 fire events. Twelve of the fires had SNI >3.0 (mean peak magnitude = 11.096 particles cm^{-2} yr^{-1}). FI 2 was short-lived

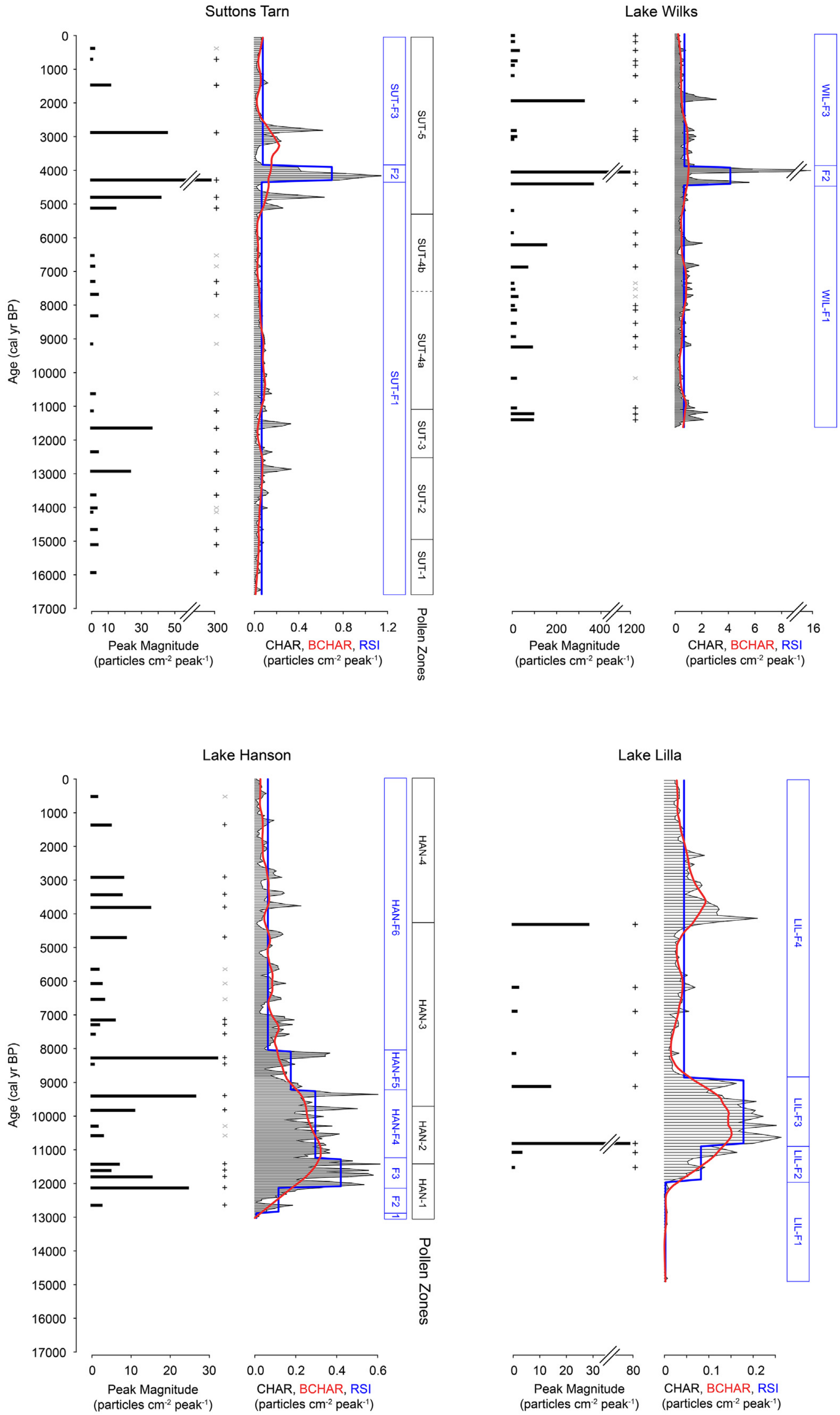

Fig. 6. Charcoal data from Cradle Mountain sites. Charcoal accumulation rates (CHAR; gray histogram), background CHAR (red line), charcoal peaks (signal-to-noise ratio >3.0 = black +, signal-to-noise ratio <3.0 = gray ×), and peak magnitude (black bars) were determined using CharAnalysis (Higuera et al., 2009). Blue lines indicate shifts in CHAR as determined by regime-shift index algorithm (RSI; Rodionov, 2004). Fire Interval (FI) as determined by RSI shown in blue boxes above each site plot. Pollen zones for Lake Hanson and Suttons Tarn shown in black boxes (see Figs. 4 and 5). (For interpretation of the references to colour in this figure legend, the reader is referred to the web version of this article.)

(18.5–16.5 cm depth; 4320–3870 cal yr BP) but had very high CHAR values (mean CHAR = 0.698 particles cm^{-2} yr^{-1}). The single fire identified in this period had the highest magnitude of any event in the record (272.64 particles cm^{-2} yr^{-1} at 18.5 cm depth; 4290 cal yr BP). FI 3 (16.5–0.0 cm depth; 3870– −62 cal yr BP) had a mean CHAR value of 0.075 particles cm^{-2} yr^{-1}, and four fires were identified (three with SNI > 3.0; mean peak magnitude = 18.61 particles cm^{-2} yr^{-1}).

4.3.5. Composite charcoal record

The four charcoal records and that from Wombat Pool (Stahle et al., 2016), representing 1497 individual charcoal samples, were used to build the composite charcoal record and estimate trends in fire activity. The preferred model explained 42% of the variance (Table 4).

5. Discussion

5.1. Fire & vegetation history of Cradle Mountain

5.1.1. Late-glacial period (ca. 17,000–14,500 cal yr BP)

Following deglaciation, open vegetation was widespread in Cradle Mountain. Pollen data from Suttons Tarn and Wombat Pool indicate grasses and herbaceous plants were dominant (Figs. 4 and 5). Fire activity was extremely low during this period (Figs. 6 and 7).

5.1.2. Transition from late glacial to early Holocene (ca. 14,500–11,500 cal yr BP)

Forest taxa expanded their range after ca. 14,500 cal yr BP. *Phyllocladus*, which serves as an early successional rainforest tree and also grows in mixed forest, became important at this time. A so-called *Phyllocladus* "bulge" is evident at other montane sites in western Tasmania (Beck et al., 2017; Macphail, 1979), and at all three pollen records from Cradle Mountain. It occurred between ca. 13,000–12,000 cal yr BP at L. Hanson, ca. 15,000–12,000 cal yr BP at Suttons Tarn, and ca. 15,000–14,000 cal yr BP at Wombat Pool (Stahle et al., 2016). The L. Hanson sediment core extends only to 13,000 cal yr BP; thus, the oldest date for the *Phyllocladus*-dominated forest at that site may not reflect its local establishment. The early decline of the *Phyllocladus* forest at Wombat Pool may have been a consequence of the site's open exposed setting, which would have enabled woody shrub taxa, such as *Leptospermum-Baeckea*, *Melaleuca*, and Proteaceae, to colonize and compete with *Phyllocladus* earlier on.

Fire activity was low through most of this transitional period and increased markedly at the beginning of the Holocene. Lake Hanson and Suttons Tarn record an initial uptick in fire at ca. 13,000 cal yr BP (Fig. 6). The increase was short-lived at Suttons Tarn. At ca. 12,000 cal yr BP, Lake Hanson, Lake Lilla, and Wombat Pool experienced sharp increases in biomass burning (Figs. 6 and 7).

5.1.3. Early Holocene (ca. 11,500–9000 cal yr BP)

The increase in fire activity at Lake Hanson, Lake Lilla, and Wombat Pool continued into the early-Holocene period until ca. 9500 cal yr BP. Prior to 11,000 cal yr BP, fire activity was slightly elevated at Suttons Tarn and Lake Wilks as well, but comparatively lower than at the other three sites (Figs. 6 and 7). These two sites are situated in smaller, topographically protected basins and at a higher elevation than the other three. Lake Wilks and Suttons Tarn have steep slopes around their basins, with rocky ridges and shallow soils (Fig. 1E; Thrush, 2008). The protected settings and higher elevation of L. Wilks and Suttons Tarn compared with L. Hanson, L. Lilla, and Wombat Pool likely explain the relatively low CHAR levels during the early Holocene. Fires were smaller in these basins and fuel biomass was lower, but small increases were recorded in both.

At Wombat Pool and Lake Hanson (and presumably Lake Lilla given its close proximity to Wombat Pool), an increase in shrubs, such as *Leptospermum-Baeckea*, *Banksia*, *Tasmannia lanceolata*, Ericaceae, and *Podocarpus lawrencii*, likely contributed to the increase in biomass burning given their high flammability and rapid post-fire regeneration. The relatively high pollen percentages of *Gymnoschoenus sphaerocephalus* during this period at Wombat Pool and L. Hanson may have also been important in driving higher fire activity. *G. sphaerocephalus* is a pyrophytic tussock-forming sedge that vigorously regenerates after fire (Burrows, 2002; Pyrke and Marsden-Smedley, 2005). In addition, *N. cunninghammii* pollen was present in values > 40% at L. Hanson and Wombat Pool (Stahle et al., 2016), but not at L. Wilks (Chin and Haberle, 2013) or Suttons Tarn. The site differences suggest that *N. cunninghammii* was locally present but restricted to elevations below ca. 1000 m in Cradle Mountain at this time. The high CHAR suggests higher levels of burning at low elevations, supported by a mosaic of pyrophytic sclerophyllous shrubs and rainforest trees. This fuel mosaic may partially explain the higher CHAR in these lakes, inasmuch as fires started in woody vegetation and/or *G. sphaerocephalus* sedgeland would have burned to the edge of temperate rainforest patches before being extinguished due to microclimate differences in flammability (e.g. Wood et al., 2011; Tepley et al., 2016). The pollen record from Suttons Tarn indicates an increase in shrubs in the catchment (particularly Ericaceae) at this time as well, but the locally dominant taxon during this period, *N. gunnii*, suggests the presence of a shorter-statured subalpine rainforest with substantially less biomass than the taller rainforest patches at lower elevations. These differences in vegetation composition, along with topographic factors, explain the differences between the charcoal records from Wombat Pool, Lakes Hanson and Lilla and those from the higher elevation sites, Suttons Tarn and Lake Wilks.

5.1.4. Mid-Holocene (ca. 9000–4500 cal yr BP)

A prolonged period of rainforest dominance characterized the mid-Holocene vegetation in Cradle Mountain. Herbaceous and sclerophyll woodland taxa declined to their lowest percentages of the Holocene and cool temperate rainforest taxa, especially *N. cunninghammii* and *N. gunnii*, reached their maximum. This period of maximum rainforest has been noted in other pollen records from western Tasmania (e.g. Colhoun, 1996; Macphail, 1979; Markgraf et al., 1986), although the extent of wet forest is debated. A recent reconstruction of past vegetation within a 50-km radius of Dove Lake (see Fig. 1), based on modern pollen calibration (using the REVEALS program), suggests that approximately half of the vegetation cover during the mid-Holocene was rainforest and the rest was a mix of non-forest types including shrubland, grassland, and sedgeland (Mariani et al., 2017). Fletcher and Thomas (2007b) also note that the primary rainforest taxa produce different amounts of pollen. Pollen of *N. cunninghammii* and *P. aspleniifolius* is over-represented in surface samples in relation to their abundance in the forest, whereas pollen of two other rainforest dominants, *N. gunnii* and *Athrotaxis-Diselma*, is underrepresented (Table 3). The mid-Holocene rainforest maximum period was expressed by high percentages of *N. cunninghammii*, *N. gunnii*, and *Athrotaxis-Diselma* but was variable across the three sites. The two underrepresented taxa, *N. gunnii* and *Athrotaxis-Diselma*, had high pollen percentages at Suttons Tarn (median = 37%), moderate amounts at Lake Hanson (median = 15%) and lower amounts at Wombat Pool (median = 8.5%). Based on our understanding of the modern pollen rain, these differences imply more rainforest cover at higher elevations and a mix of open vegetation and rainforest vegetation at lower elevations. Local topography and edaphic

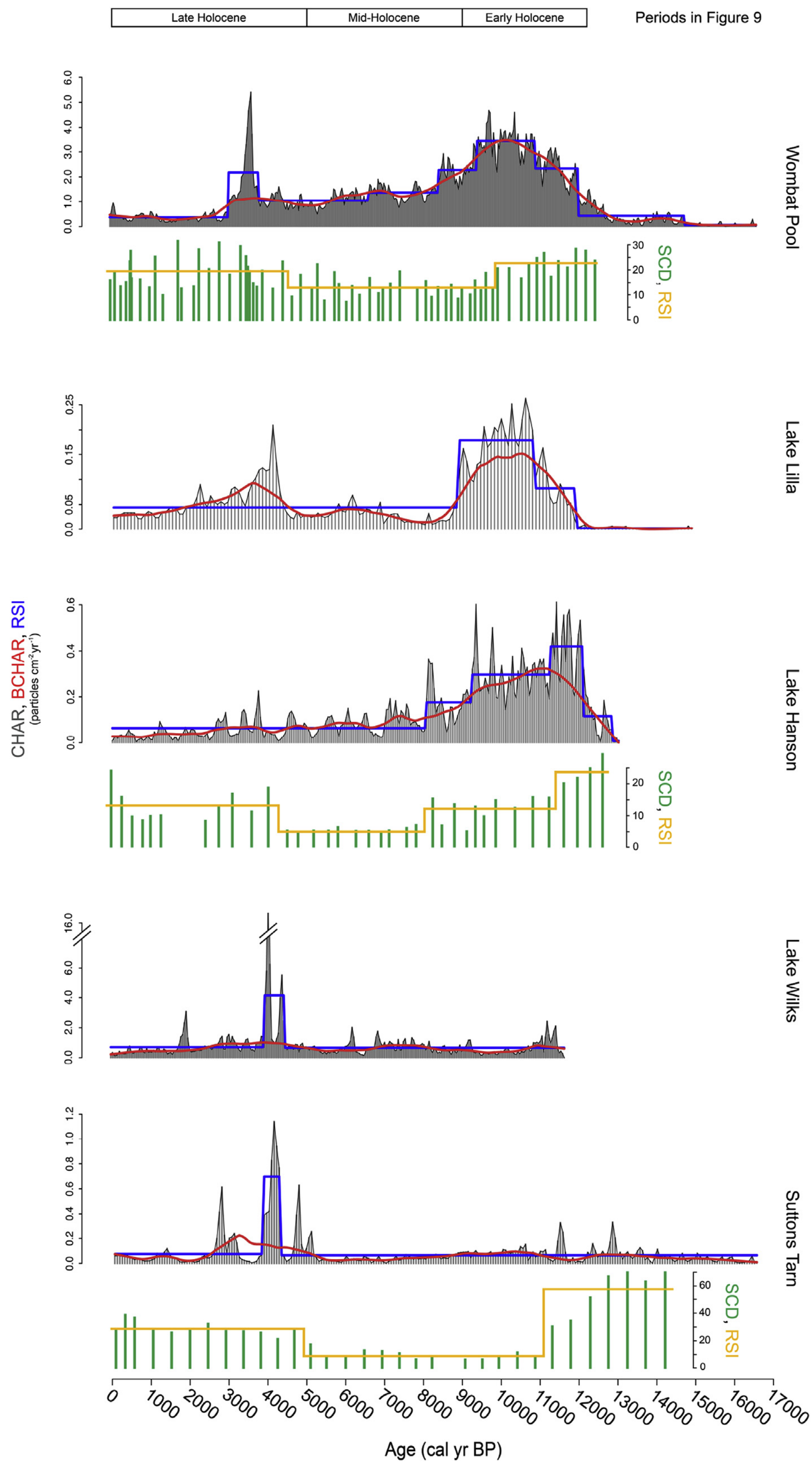

Fig. 7. Fire and vegetation summary for Cradle Mountain sites. Charcoal accumulation rate (CHAR; gray histograms), background CHAR (red lines), and regime shift index (RSI; blue lines) for the five charcoal records from Cradle Mountain. Square chord distance (SCD; green bars) and RSI (yellow lines) for each of the three pollen records from the Cradle Mountain region. For SCD, the lower the number the more similar the sample is to a temperate rainforest assemblage; the higher the number the more different the pollen sample is from a temperate rainforest assemblage. (For interpretation of the references to colour in this figure legend, the reader is referred to the web version of this article.)

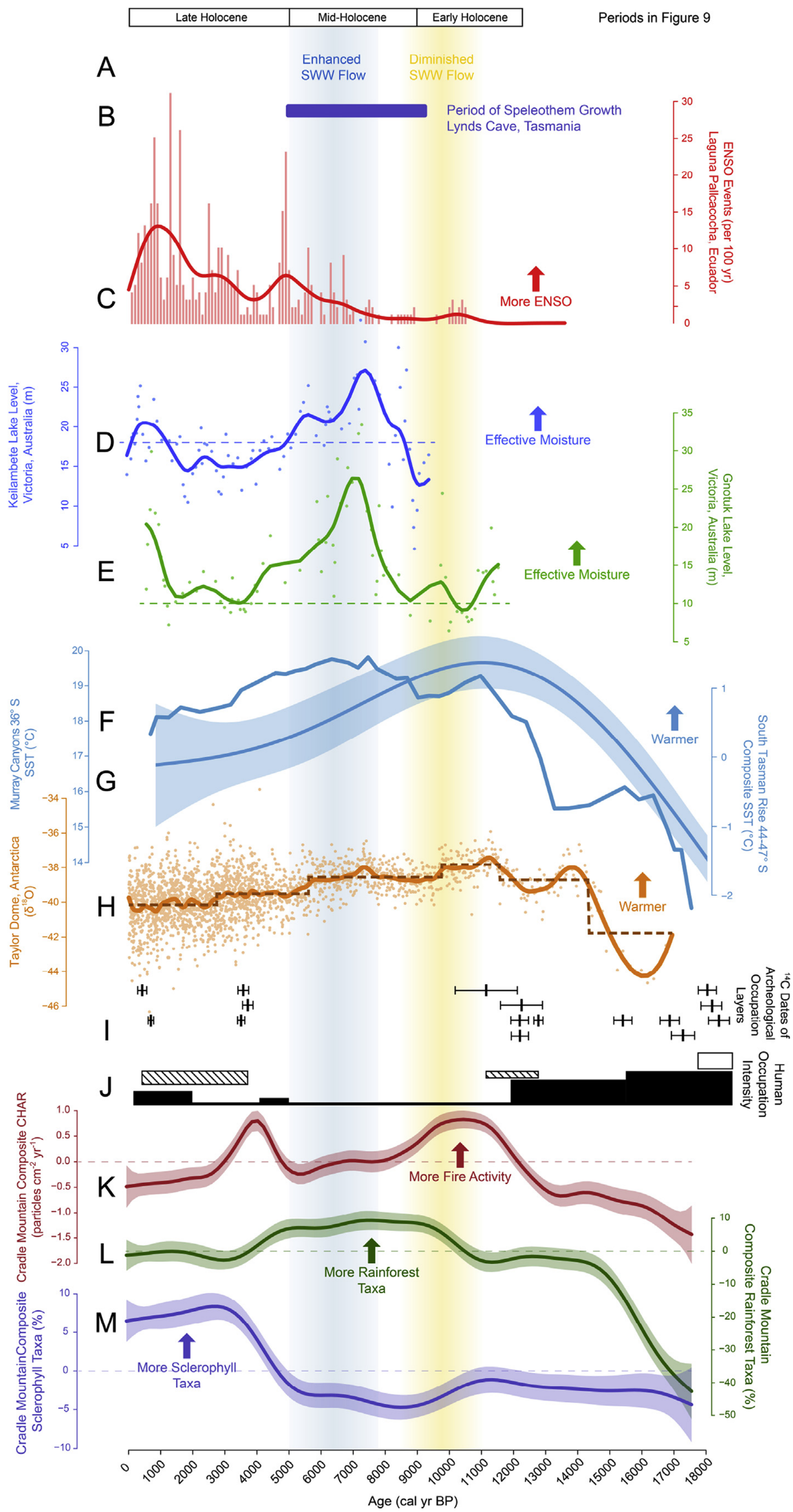

Late Holocene
Mid-Holocene
Early Holocene
Periods in Figure 9
A
Enhanced SWW Flow
Diminished SWW Flow
B
Period of Speleothem Growth Lynds Cave, Tasmania
C
More ENSO
ENSO Events (per 100 yr) Laguna Pallcacocha, Ecuador
D
Kailambete Lake Level, Victoria, Australia (m)
Effective Moisture
E
Effective Moisture
Gnotuk Lake Level, Victoria, Australia (m)
F
G
Murray Canyons 36° S SST (°C)
Warmer
South Tasman Rise 44-47° S Composite SST (°C)
H
Taylor Dome, Antarctica ($\delta^{18}O$)
Warmer
I
^{14}C Dates of Archeological Occupation Layers
J
Human Occupation Intensity
K
Cradle Mountain Composite CHAR (particles cm^{-2} yr^{-1})
More Fire Activity
L
More Rainforest Taxa
Cradle Mountain Composite Rainforest Taxa (%)
M
More Sclerophyll Taxa
Cradle Mountain Composite Sclerophyll Taxa (%)
Age (cal yr BP)

factors were also an important control of rainforest distribution, with south-facing fire-protected slopes likely supporting more pyrophobic taxa (Fletcher et al. *in review*) and the exclusion of trees in waterlogged areas (Fletcher et al., 2014b). Such conditions may explain why more rainforest vegetation was present at Suttons Tarn during the mid-Holocene. Fire activity in Cradle Mountain during this period was greatly reduced from the early Holocene (Figs. 6 and 7) and the magnitude of fire events was much lower than in the early and late Holocene (Fig. 6; Stahle et al., 2016).

5.1.5. Late Holocene (ca. 4500 cal yr BP–present)

The pollen data show a substantial change in vegetation in the late Holocene. Much of the closed rainforest of the mid-Holocene was replaced by open sclerophyll woodland across large swaths of Cradle Mountain as evidenced by a sharp increase in sclerophyll taxa, especially *Eucalyptus* at all three sites (Figs. 4 and 5; Stahle et al., 2016). Rainforest and subalpine taxa, particularly *N. gunnii*, *Athrotaxis-Diselma*, and *N. cunninghammii*, declined in the pollen records of all three sites between ca. 5200-4000 cal yr BP (Figs. 4 and 5; Stahle et al., 2016). Sclerophyll woodland shrubs, including *Monotoca*, *Ericaceae*, *Casuarina*, Proteaceae, and *Leptospermum-Baeckea*, as well as herbaceous taxa increased at this time. Small increases in shorter-lived rainforest and wet sclerophyll taxa, such as *Pomaderris*, *Anodopetalum-Eucryphia* and *Dicksonia antarctica*, occurred as well. This shift indicates the development of mixed forests that contain wet sclerophyll and rainforest species during the late Holocene. Finally, at Suttons Tarn, the highest elevation site, subalpine shrubs increased in addition to increases in *Eucalyptus* and other sclerophyll taxa, while *N. gunnii* declined substantially. Many other western Tasmanian sites record a shift away from rainforest and subalpine taxa toward sclerophyllous taxa in the late Holocene, including at Dove Lake (Mariani et al., 2017), Lake St Clair (Hopf et al., 2000), Beatties Tarn, Eagle Tarn, Tarn Shelf (Mount Field; Macphail, 1979), Lake Osborne (Hartz Mountains; Fletcher et al., 2014a), and Paddy's Lake (Beck et al., 2017).

All five charcoal records from Cradle Mountain display a dramatic increase in fire occurrence between ca. 4800-3600 cal yr BP (Figs. 6 and 7). At Lake Wilks, Suttons Tarn, and Wombat Pool, the largest fire event occurred during this interval and a fire-regime shift was also recorded (Fig. 6; Stahle et al., 2016). Our charcoal records are of higher temporal resolution than our pollen records making it difficult to assess the role of fire in the establishment of open sclerophyll-dominated woodland. At Lake Osborne in the Hartz Mountains of southwest Tasmania, it has been suggested that the late-Holocene shift to sclerophyll woodland was driven by recurrent fires between ca. 2900-2600 cal yr BP (Fletcher et al., 2014a). In Cradle Mountain and at Lake Vera (Fletcher et al., *in review*), the shift from rainforest and subalpine communities toward sclerophyll woodland was more gradual and the increase in *Eucalyptus* woodland preceded the increase in late-Holocene fire episodes but that fires likely catalyzed the vegetation transition (Supplemental Fig. 2).

5.2. Climate and human influences

Paleoenvironmental reconstructions suggest that changes in fire activity and vegetation over time are related to variations in both top-down climate and bottom-up fuel-related controls. For each time period, independent proxy evidence of large-scale changes in climate and human activity is compared with the fire and vegetation history in the Cradle Mountain region to evaluate the relative importance of drivers of past ecological change.

Three well-studied archeological sites are situated within ca. 25 km of Cradle Mountain: Mackintosh Cave, Warragarra Rockshelter, and Parmerpar Meethaner Rockshelter (Fig. 1D). Analyses of these sites have characterized human occupation in two ways: (1) radiocarbon dates on occupation layers—strata that contain human-made tools and animal bones with evidence of human butchery, and (2) discard rates—the number and kind of discarded bones and tools throughout the archeological deposits (Allen and Porch, 1996; Cosgrove, 1995; Lourandos, 1983; Stern and Marshall, 1993). Not every occupation layer has been radiocarbon dated so discard rates fill in the gaps between dates as well as provide more information about how and with what intensity sites were used over time (Cosgrove, 1999; Jones, 1995). While the short-term influences of people in igniting and facilitating fire occurrence cannot be assessed, it is useful to compare broad periods of human activity with fire-history trends.

The three archeological sites discussed here were first occupied in the Pleistocene and the most intense periods of use at Parmerpar Meethaner and Mackintosh Cave pre-date the paleoenvironmental record from Cradle Mountain. Parmerpar Meethaner Rockshelter is the second oldest archeological site yet discovered in Tasmania with a basal age of 38,111 ± 1207 cal yr BP (33,850 ± 450 ^{14}C BP; Cosgrove, 1995). Moderate to high levels of human use were recorded between ca. 23,000–12,000 cal yr BP with the highest levels between ca. 19,000–15,000 cal yr BP. Mackintosh Cave recorded a period of intense human occupation between ca. 21,000–17,500 cal yr BP (Stern and Marshall, 1993). The record from Warragarra Rockshelter begins ca. 12,000 cal yr BP.

5.2.1. Late-glacial period (ca. 17,000–14,500 cal yr BP)

Deglaciation occurred between 18,000 and 16,000 cal yr BP in Tasmania (Barrows et al., 2002; Mackintosh et al., 2006). Of the five records, only Suttons Tarn and Wombat Pool predate 15,000 cal yr BP. Their pollen and charcoal records suggest an initial landscape dominated by grasses and herbs and very few fires. Climate proxy data indicate cool conditions during this period. Antarctic air temperatures, as recorded by δ^{18}O values, were low (EPICA Members, 2004; Grootes et al., 2001, Fig. 8H). Regional sea-surface

Fig. 8. Comparison of climate and archeological data to Cradle Mountain fire and vegetation data. (A) Periods of enhanced and diminished Southern Hemisphere Southwesterly Winds (SWW) strength in the Tasmanian sector (summarized from Fletcher and Moreno, 2012; Rees et al., 2015). (B) Stalagmite growth record from Lynds Cave, Tasmania. This record spans 5000–9200 cal yr BP (Xia et al., 2001). (C) The number of El Niño events per 100 years (Moy et al., 2002) with smoothing spline (spar = 0.6). (D, E) Modeled reconstructions of lake depths relative to modern (dashed lines) for Lake Keilambete (blue) and Lake Gnotuk (green) in southern Victoria, Australia (Wilkins et al., 2013). (F) Alkenone-derived sea surface temperature (SST) reconstruction from marine core MD03-2611 at Murray Canyons off the coast of South Australia (Calvo et al., 2007). (G) Composite SST record from four sites (GC07, GC14, GC17, and GC31) south of Tasmania between 44 and 47° S latitude. Trends in SST were estimated by a GAM applied to alkenone-derived SST data and MAT-derived (modern analog technique) SST data (78 total samples from Sikes et al., 2009; standard errors are shown in light blue; see Table 4). (H) Oxygen isotope ratios from Taylor Dome, Antarctica (Grootes et al., 2001) with smoothing spline (orange; spar = 0.6) and regime shifts (dark orange dashed line; regime shift determined using algorithm from Rodionov, 2004). (I) The 1σ calibrated age range of ^{14}C dates on occupation layers at three archeological sites within ~25 km of Cradle Mountain (Warragarra Rockshelter, Parmerpar Meethaner Rockshelter, Mackintosh Cave). (J) Inferred occupation intensity from the three archeological sites within ~25 km of Cradle Mountain based on artefact discard rates and sediment accumulation rates (Warragarra Rockshelter = white bars with diagonal lines (Allen and Porch, 1996), Parmerpar Meethaner Rockshelter = black bars (Cosgrove, 1995), Mackintosh Cave = white bar (Stern and Marshall, 1993)). (K) Composite fire-history record from the Cradle Mountain region. Trends in fire activity were estimated by GAMs applied to the charcoal influx data (n = 1497; standard errors are shown in light shading). (L, M) Composite rainforest (green) and sclerophyll (purple) taxa from the Cradle Mountain region. Trends in pollen taxa were estimated by GAMs applied to the pollen percent data (n = 163; standard errors are shown in light shading). (For interpretation of the references to colour in this figure legend, the reader is referred to the web version of this article.)

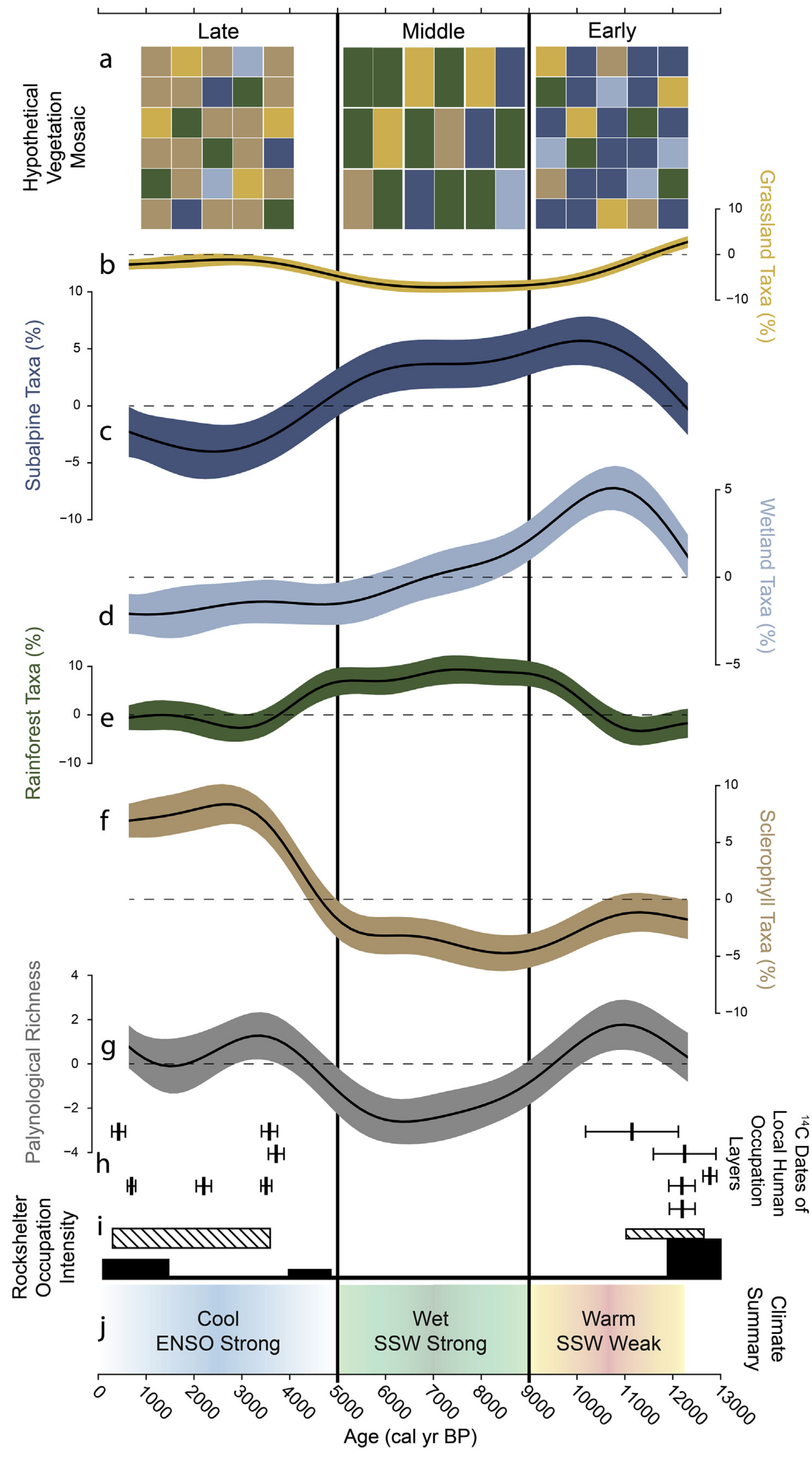

Fig. 9. Summary pollen, charcoal, & archeological data. a) Hypothetical vegetation mosaic for early, mid- and late Holocene periods. b) Composite grassland taxa. c) Composite subalpine taxa. d) Composite wetland taxa. e) Composite rainforest taxa. f) dates on occupation layers at two archeological sites within ~25 km of Wombat Pool. i) Occupation intensity at the two archeological sites (Warragarra Rockshelter = white bars with diagonal lines, Parmerpar Meethaner Rockshelter = black bars) as measured by artifact discard rates (Cosgrove, 1995; Allen and Porch, 1996). The height of the bar corresponds to inferred occupation intensity, i.e. the higher the bar, the higher the intensity. Note Parmerpar Meethaner had continuous occupation through the Holocene mostly at very low levels, and a prolonged hiatus in occupation was recorded at Warragarra. j) Climate summary with dominant parameter and driver indicated. The trends in pollen (b-f) were estimated by GAMs applied to the pollen percent data (n = 163; black lines = mean; shading = standard errors).

temperatures (SSTs) were also relatively low compared with Last Glacial Maximum (LGM) values. Alkenones and faunal assemblages in marine cores from south (44–47° S) and northwest (36° S) of Tasmania indicate SSTs were higher than the LGM but lower than Holocene levels (Calvo et al., 2007; Sikes et al., 2009, Fig. 8F; G).

Warragarra and Parmerpar Meethaner rockshelters were used by humans during this period. The archeological evidence from Warragarra Rockshelter suggests a period with low levels of occupation at ca. 12,000 cal yr BP (Allen and Porch, 1996; Lourandos, 1983, Fig. 8J). Parmerpar Meethaner contains evidence of high human use (Cosgrove, 1995, Fig. 8J). The negligible levels of charcoal in the lake records prior to 12,000 cal yr BP may have been a result of cool conditions, discontinuous fuel cover, and/or low levels of deliberate burning.

5.2.2. Transition from the late-glacial to early Holocene (ca. 14,500–11,500 cal yr BP)

The decline of herbaceous plants and increase in *Phyllocladus*-dominated forest were likely aided by warming during this transitional period. Antarctic air temperature increased after ca. 14,500 cal yr BP (Grootes et al., 2001, Fig. 8H) while regional SSTs rose rapidly at ca. 13,500 cal yr BP (Calvo et al., 2007, Fig. 8F). The charcoal data suggest that levels of biomass burning steadily increased after 13,000 cal yr BP (Fig. 8J). Warming temperatures and more continuous fuel cover likely increased fire activity in Cradle Mountain, although humans may have served as an ignition source.

Warragarra Rockshelter was apparently used as a transient hunting base (Lourandos, 1983), whereas Parmerpar Meethaner Rockshelter was consistently used from 15,000–12,000 years ago but less intensively than during the previous 4000 years (Cosgrove, 1995). As the climate warmed, use of resources at higher elevations in the Cradle Mountain area increased and deliberate burning may have contributed to higher levels of biomass burning after ca. 13,000 cal yr BP that cannot be inferred from the archeological evidence. Warming and increased fuel cover would have favored fire (e.g. Whitlock et al., 2007), and humans may have provided ignitions, especially after 13,000 cal yr BP when charcoal values were high.

5.2.3. Early Holocene (ca. 11,500–9000 cal yr BP)

Charcoal data suggest that the period from ca. 11,200–9800 cal yr BP had the highest levels of burning in the Cradle Mountain region (Fig. 8J), and regional climate data indicate that this period was warm and dry. Antarctic temperatures at Taylor Dome reached their highest between ca. 11,500–9500 cal yr BP (Grootes et al., 2001, Fig. 8H). SSTs south of Tasmania exhibited steady increase throughout the postglacial period and reached a maximum at ca. 11,000 cal yr BP (Sikes et al., 2009, Fig. 8G), and SSTs northwest of Tasmania were also high at this time (Calvo et al., 2007, Fig. 8F). A lake-level reconstruction from Lake Gnotuk in southern Victoria, Australia, indicates low water levels in the early Holocene consistent with low effective moisture (Wilkins et al., 2013, Fig. 8E). At the latitude of northern Tasmania, the strength of the Southern Hemisphere Westerly Winds (SWW) also diminished in the early Holocene (Fig. 8A) based on chironomid, geoelemental, and grain size data from southern Tasmania (Rees et al., 2015), as well as a synthesis of lake-level changes and reconstructed precipitation trends from the Southern Hemisphere mid-latitude (Fletcher and Moreno, 2012).

The archeological record from the Cradle Mountain region includes two ^{14}C dates from Warragarra Rockshelter from the early Holocene. The dates were derived from bulk sediment prior to AMS radiocarbon dating and the 1-sigma error margins are large (>1500 years; Fig. 8I). The conclusion from two archeological surveys was that the use of Warragarra was short-lived and centered on ca. 12,000 cal yr BP (Allen and Porch, 1996; Lourandos, 1983). No occupation layers have been radiocarbon dated from Mackintosh Cave or Parmerpar Meethaner Rockshelter during this period (Fig. 8I). The artifact discard record from Parmerpar Meethaner indicates an abrupt decline in human use of the site at ca. 12,000 cal yr BP (Cosgrove, 1995, Fig. 8J). The lack of a clear archeological signal, while not definitive, suggests that increased temperature and lower effective moisture coupled with increases in biomass, particularly shrubs, were likely drivers of elevated levels of fire during this period.

5.2.4. Mid-Holocene (ca. 9000–4500 cal yr BP)

Paleoclimate evidence suggests a relatively wet period that was as warm or slightly less warm than the early Holocene. At Lynds Cave, 25 km northwest of Cradle Mountain, a period of speleothem growth from 9200 to 5000 cal yr BP implies higher effective moisture at this time (Xia et al., 2001; Zhao et al., 2001, Fig. 8B). High water levels at lakes Keilambete and Gnotuk in Victoria indicate a widespread increase in precipitation was a regional phenomenon. These records show a synchronous rise in the mid-Holocene with a Holocene high-stand at ca. 7200 cal yr BP (Wilkins et al., 2013, Fig. 8D; E). Furthermore, multiple lines of evidence indicate SWW flow was enhanced in the Tasmanian sector between ca. 8000-5000 cal yr BP (Fletcher and Moreno, 2011, 2012; Rees et al., 2015, Fig. 8A). Storm tracks would have delivered more precipitation to the Cradle Mountain region, than in the early Holocene when the SWW flow was weak at this latitude. The evidence for relatively warm conditions in the mid-Holocene includes an ocean record northwest of Tasmania at Murray Canyons, which indicates maximum SSTs at ca. 7500 cal yr BP followed by warm but declining SSTs (Calvo et al., 2007, Fig. 8F). The Taylor Dome $\delta^{18}O$ record indicates temperatures were slightly lower than the early-Holocene maximum but still elevated in the mid-Holocene (Grootes et al., 2001, Fig. 8H). Summer temperatures at Mount Field were reconstructed from chironomids at two sites that disagree on the timing of the Holocene thermal maximum—ca. 6700 cal yr BP and ca. 4500 cal yr BP (Rees and Cwynar, 2010). The composite record of four SST records from lat. 44–47°S indicates a steady decline after a Holocene thermal maximum at ca. 11,000 cal yr BP (Sikes et al., 2009, Fig. 8G). On balance, the paleoclimate evidence indicates that Tasmania was warm and had high effective moisture in the early Holocene. High effective moisture explains the temperate rainforest expansion recorded at several sites in western Tasmania (e.g. Beck et al., 2017; Colhoun, 1996; Hopf et al., 2000; Macphail, 1979; Mariani et al., 2017; Markgraf et al., 1986), and the reduced fire activity recorded in and around Cradle Mountain (our records; Mariani et al., 2017; Fletcher et al. *in review*; Beck et al., 2017).

Between ca. 10,000 and 4000 cal yr BP, the absence of radiocarbon-dated artifacts from the three archeological sites in the Cradle Mountain region (Fig. 8I) suggests minimal or low-intensity use. Artifact discard rates indicate that Parmerpar Meethaner Rockshelter was used during the mid-Holocene but less so than during the late-glacial period (Cosgrove, 1995, Fig. 8J). Across western Tasmania, archeological evidence suggests that many caves and rockshelters were abandoned (Cosgrove, 1999), possibly as a result of inhospitable living conditions during this period of increased effective moisture (e.g. Thomas, 1991). The archeological evidence, however, places the decline and cessation of use of Warragarra Rockshelter, Mackintosh Cave and Parmermar Meethaner Rockshelter at ~1800–2800 years before the paleoclimate data indicate the onset of wet conditions. People may have remained in the Cradle Mountain region throughout the mid-Holocene and employed subsistence strategies that made little use of rockshelters (Cosgrove, 1999; Pike-Tay et al., 2008; Thomas, 1993). The lower fire activity at this time, in any case, suggests reduced ignitions.

5.2.5. Late Holocene (ca. 4500 cal yr BP–present)

The replacement of long-lived rainforest trees by herbaceous plants, woodland shrubs, and shorter-lived rainforest trees, and wet sclerophyll understory trees, tree ferns, and shrubs (i.e. *Pomaderris apetala*, *Dicksonia antarctica*, *Anodopetalum-Eucryphia*) in the late Holocene is consistent with evidence of a more variable climate after ca. 6000-5000 cal yr BP. Increased climate variability was possibly a result of the onset and/or strengthening of ENSO (McGlone et al., 1992; Moy et al., 2002; Shulmeister and Lees, 1995; Wanner et al., 2008, Fig. 8C) leading to La Niña (wet) and El Niño (dry) states in western Tasmania (Marx et al., 2009). Fluctuations in vegetation composition and/or fire occurrence are observed at many sites in the late Holocene and attributed to increased climate variability (i.e. Beck et al., 2017; Fletcher et al., 2014a, 2015; Haberle, 2005; Donders et al., 2007; McWethy et al., 2016; Rees et al., 2015). Overall, regional climate conditions were cooler and drier in the late Holocene than in the early and mid-Holocene. Speleothem growth ceased at 5000 cal yr BP at Lynds Cave, indicating lower effective moisture after this time (Xia et al., 2001, Fig. 8B). Lake levels in Victoria declined from the mid-Holocene high stand and were low between ca. 5000-1000 cal yr BP (Wilkins et al., 2013, Fig. 8D; E). Regional SSTs declined from early/mid-Holocene maxima indicating cooling (Calvo et al., 2007; Sikes et al., 2009, Fig. 8F; G), and the Taylor Dome record exhibits slowly declining temperature after ca. 8000 cal yr BP and increased variability after ca. 5000 cal yr BP (Grootes et al., 2001, Fig. 8H).

Archeological evidence from Warragarra and Parmerpar Meethaner rockshelters suggests modest levels of human occupation after ca. 3900 cal yr BP (Fig. 8I and J). The number of artifacts is lower at Parmerpar Meethaner than in the early postglacial period (Cosgrove, 1995), whereas intermittent use of Warragarra was a feature of the late-glacial, early Holocene and late Holocene (Allen and Porch, 1996; Lourandos, 1983). The increased presence of people in the last 3900 years could have provided an ignition source that was lacking in the mid-Holocene. However, the large area impacted by fire in the late Holocene in Cradle Mountain is inconsistent with what is known about the targeted and strategic manner in which Aboriginal peoples employed fire in Tasmania and other parts of Australia (Bird et al., 2008; Gammage, 2008, 2011; Gott, 2005; Marsden-Smedley and Kirkpatrick, 2000; Trauernicht et al., 2015).

5.3. Holocene vegetation and land-use strategies: past human-fire interactions

The pollen records from Wombat Pool, Lake Hanson, and Suttons Tarn exhibit a very similar pattern during the Holocene. All sites show a multi-millennial phase of protracted rainforest in the mid-Holocene, whereas vegetation was more open in the early and late Holocene (Fig. 7). The difference in the timing of vegetation shifts at each site corresponds with changes in local fire activity. Lake Hanson displays two stepwise shifts in the early Holocene at ca. 11,400 cal yr BP and ca. 8150 cal yr BP. Both shifts are associated with a decline in fire activity (Fig. 7). Likewise, the pollen data at Suttons Tarn suggest a shift toward rainforest after the charcoal record registers a decline in fire activity at ca. 11,000 cal yr BP (Fig. 7). Wombat Pool also records a vegetation shift at ca. 9800 cal yr BP (Fig. 7), although this predated a decline in local fire activity by ~200 years. All three sites record a prolonged period of more rainforest in the mid-Holocene, followed by a shift toward wet sclerophyll woodland in the late Holocene between 4900 and 4300 cal yr BP (Fig. 7). The early- and late-Holocene assemblages were more similar to one another than they were to the mid-Holocene assemblages (Fig. 7).

In addition to the relationship between vegetation composition (as measured by SCD) and fire activity (as measured by CHAR), a close correspondence is evident between fire and floristic diversity (as measured by palynological richness) (Fig. 9). The early-Holocene fire maximum (ca. 11,800–9800 cal yr BP) coincided with an increase in sclerophyll and subalpine taxa and high palynological richness. Maximum temperate rainforest expansion between ca. 8500 and 5500 cal yr BP was associated with declining palynological richness. The lowest palynological richness was recorded at the end of this period ca. 6000 cal yr BP, which also featured low fire activity. An abrupt increase in fire at ca. 4800-3200 cal yr BP was accompanied by pollen increases in sclerophyll taxa, declines in rainforest taxa, and high palynological richness values.

This relationship suggests that periods of elevated levels of burning were associated with high floristic diversity in Cradle Mountain (Fig. 9). Increased palynological richness in the early Holocene resulted from more sclerophyllous and subalpine taxa while the late-Holocene rise in palynological richness was primarily driven by an increase in sclerophyll taxa (Fig. 9).

The patterns evident in the SCD and palynological richness data suggest changes in spatial heterogeneity of vegetation during the early, mid- and late Holocene. The pollen data indicate that, during the mid-Holocene, the Cradle Mountain region supported a more coarse-grained mosaic, particularly at higher elevations, creating a more homogeneous vegetation structure and composition than existed previously or at present. The pollen records suggest the present fine-grained mosaic of rainforest, wet sclerophyll woodland, mixed forest, sedgeland, sclerophyll scrub, grassland, and subalpine forest, and shrubland communities developed ca. 4600 cal yr BP in association with increasing climate variability. Based on the pollen records and SCD analysis, the early-Holocene vegetation also featured a fine-grained mosaic of rainforest, mixed forest, open woodland, shrubland, sedgeland, and grassland (Fig. 9). The differences between the three Holocene periods are best explained by climate. Warming in the early Holocene facilitated an expansion of forest and shrub communities, while the relatively aridity of this period likely restricted rainforest to isolated wetter microclimates. The wetter conditions of the mid-Holocene, in contrast, favored expansion of temperate rainforest and a more coarse-grained vegetation structure. The drier, more variable conditions of the late Holocene supported a return to a more-patchy vegetation structure.

The much-debated questions of whether, how, and when Aboriginal Tasmanians may have altered landscapes through their use of fire cannot be answered with charcoal, pollen, and archeological data alone. People have undoubtedly influenced vegetation and disturbance regimes at some level over that last 40,000 years (Kershaw et al., 2007; Fletcher and Thomas, 2010a). Our focus is on factors responsible for broad changes in vegetation history during the last 14,000 years following deglaciation. The Cradle Mountain records, like others in Tasmania, point to climate as the primary driver of postglacial vegetation change, but Aboriginal land-use practices likely reinforced the effects of climate. The fine-grained heterogeneous vegetation mosaic that developed in the early and late Holocene, for example, would have been more conducive to hunting strategies than a coarse-grained mosaic dominated by closed forest (Fig. 9a). Cosgrove et al. (1990) postulates that the discrete grassland patches that occurred on fertile substrates within much larger complexes of forest, shrubland and sedgeland were “ecologically tethered” resources that provided relatively predictable areas for marsupial hunting. Motivation to increase hunting success may have been promoted strategies of deliberate burning.

In the Cradle Mountain region, the timing and inferred intensity of human occupation closely align with periods of abundant grassland and sclerophyll taxa. As grassland declined in the late-glacial period, occupation at Mackintosh Cave ceased (Stern and Marshall, 1993). As grassland declined further in the early Holocene, human occupation ceased at Warragarra Rockshelter and drastically diminished at Parmerpar Meethaner (Fig. 9). In the late Holocene, sclerophyll and grassland taxa increased, human use of Warragarra Rockshelter resumed, and occupation at Parmerpar Meethaner intensified. As discussed earlier, late-Holocene increases in grassland and sclerophyll woodland were coincident with an increase in fire. Increased climate variability and aridity in the late Holocene heightened the vulnerability of rainforest to burning (Holz et al., 2015; Yospin et al., 2015). Aboriginal fire management practices may have been a response to climate-driven vegetation change and enhanced climate variability, which would have dried fuels intermittently and increased ignition success. In this case, climate shaped the template of vegetation and fire and humans took advantage of the opportunities that were created (e.g. Bush et al., 2017).

6. Conclusions

Pollen and charcoal evidence from Cradle Mountain suggests that during late-glacial period, the vegetation was largely open and fires were rare; forests were likely restricted to lower elevations. After ca. 14,000 cal yr BP, rainforest taxa and subalpine shrubs increased in abundance. Fire continued to be infrequent, with the exception of a short-lived increase at high-elevation sites—Suttons Tarn and Lake Wilks.

Maximum fire activity occurred in the early Holocene at the three lower elevation sites—Lake Hanson, Lake Lilla, and Wombat Pool—while biomass burning remained low at the higher sites. Differences in elevation, topography and basin characteristics likely resulted in climate-controlled variations in vegetation and fuel flammability. Lower sites supported larger areas of rainforest, sclerophyll woodland, and open vegetation while higher sites supported more subalpine vegetation. At the lower sites, frequent fires originating in the sclerophyll woodland would have spread into the rainforest margin, producing the large amount of charcoal observed in these records during the early Holocene.

The mid-Holocene period supported an expansion of cool, temperate rainforest and reduced fire activity in the Cradle Mountain region as well as at other sites in western Tasmania. The late Holocene marked a regional shift toward open sclerophyll woodland that is associated with increased climate variability and drought. The present vegetation mosaic has been a feature of the landscape for the last ca. 4600 years. All five Cradle Mountain sites recorded a large-scale fire event in the late Holocene between ca. 4200-3600 cal yr BP that catalyzed a decline in rainforest cover and an expansion of sclerophyll woodland.

While humans have long occupied Tasmania, changes in post-glacial fire activity were primarily shaped by variations in climate. Aboriginal peoples were likely an important ignition source in the early Holocene, when the presence of more flammable sclerophyll taxa combined with warming led to more fires. Cave and rock-shelter sites near Cradle Mountain were either abandoned or used infrequently during the mid-Holocene when it was wetter, rainforest was more widespread and fire activity was reduced. The fine-grained mosaic of rainforest, mixed forest, sclerophyll woodland, and grassland of the early and late Holocene would have facilitated hunting and foraging, regardless of whether it was natural or anthropogenic in origin.

Acknowledgements

This research was supported by National Science Foundation grant OISE-09664472 to C. Whitlock and Australian Research Council grants DP0664898 to S. Haberle DP110101950 to D.M.J.S. Bowman. We also thank Michael Fletcher and David Bowman for their intellectual contribution to this work, and Virginia Iglesias for input on an earlier draft of this manuscript. For laboratory assistance we thank C. Clayton, J. Gay, J. Giskaas, F. Hopf, E. Merrell, C. Shama, J. Stevenson and R. Whitau. We appreciative the field support provided by K. Allen, C. Burke, L. Fixico, R. Gresswell, S. Nichols, K. Saunders, M. Weingard and G. Yospin. Finally, we thank two anonymous reviewers for their constructive comments.

Appendix A. Supplementary data

Supplementary data related to this article can be found at https://doi.org/10.1016/j.quascirev.2017.09.010.

References

Allen, J., Porch, N., 1996. Warragarra rockshelter. In: Allen, J. (Ed.), Report of the Southern Forests Archaeological Project: Site Descriptions, Stratigraphies and Chronologies, vol. 1. La Trobe University Press, Melbourne, VIC, pp. 195–218.
Anker, S.A., Colhoun, E.A., Barton, C.E., Petersen, M., Barbetti, M., 2001. Holocene vegetation and paleoclimatic and paleomagnetic history from Lake johnsten, Tasmania. Quat. Res. 56, 264–274.
APSA-Members, 2007. The Australasian Pollen and Spore Atlas v1.0. Australian National University, Canberra, ACT. Available online at: http://apsa.anu.edu.au.
Barrows, T.T., Stone, J.O., Fifield, L.K., Cresswell, R.G., 2002. The timing of the last glacial maximum in Australia. Quat. Sci. Rev. 21, 159–173. https://doi.org/10.1016/S0277-3791(01)00109-3.
Beck, K.K., Fletcher, M.-S., Gadd, P.S., Heijnis, H., Jacobsen, G.E., 2017. An early onset of ENSO influence in the extra-tropics of the southwest Pacific inferred from a 14, 600 year high resolution multi-proxy record from Paddy's Lake, northwest Tasmania. Quat. Sci. Rev. 157, 164–175.
Bennett, K.D., 2009. Documentation for Psimpoll 4.27 and Pscomb 1.03. C Programs for Plotting and Analyzing Pollen Data. The 14Chrono Centre, Archaeology and Palaeoecology.
Bennett, K.D., Willis, K.J., 2001. Pollen. In: Smol, J.P., Birks, H.J.B., Last, W.M. (Eds.), Tracking Environmental Change Using Lake Sediments. Terrestrial, Algal, and Siliceous Indicators, vol. 3. Kluwer, Dordrecht, pp. 5–32.
Bird, B.R., Bird, D.W., Codding, B.F., Parker, C.H., Jones, J.H., 2008. The "fire stick farming" hypothesis: Australian Aboriginal foraging strategies, biodiversity, and anthropogenic fire mosaics. Proc. Natl. Acad. Sci. U. S. A. 105, 14796–14801.
Birks, H.J.B., Line, J.M., 1992. The use of rarefaction analysis for estimating palynological richness from Quaternary pollen-analytical data. Holocene 2, 1–10.
Blaauw, M., 2010. Methods and code for "classical" age-modelling of radiocarbon sequences. Quat. Geochronol. 5, 512–518. https://doi.org/10.1016/j.quageo.2010. 01.002.
Bowman, D.M.J.S., 1998. Tansley review no. 101: the impact of Aboriginal landscape burning on the Australian biota. New Phytol. 140, 385–410.
Bowman, D.M.J.S., Wood, S.W., Neyland, D., Sanders, G.J., Prior, L.D., 2013. Contracting Tasmanian montane grasslands within a forest matrix is consistent with cessation of Aboriginal fire management. Austral Ecol. 38, 627–638.
Bureau of Meteorology. Waldheim Station, Cradle Valley Statistics. URL: http://www.bom.gov.au/climate/averages/tables/cw_096005.shtml.
Burrows, G.E., 2002. Epicormic strand structure in Angophora, Eucalyptus and Lophostemon (Myrtaceae)—implications for fire resistance and recovery. New Phytol. 153, 111–131.
Bush, M.B., Correa-Metrio, A., Van Woesik, R., Shadik, C.R., McMichael, C.N.H., 2017. Human disturbance amplifies amazonian El niño-southern oscillation signal. Glob. Change Biol. https://doi.org/10.1111/gcb.13608.
Calvo, E., Pelejero, C., De Deckker, P., Logan, G.A., 2007. Antarctic deglacial pattern in a 30 kyr record of sea surface temperature offshore South Australia. Geophys. Res. Lett. 34, L13707. https://doi.org/10.1029/2007GL029937.
Chin, H., Haberle, S.G., 2013. Holocene Vegetation and Fire History at Lake Wilks. Poster, Tasmania.
Clark, J.S., 1988. Particle motion and the theory of charcoal analysis: source area, trans- port, deposition, and sampling. Quat. Res. 30, 67–80. https://doi.org/10.1016/0033-5894(88)90088-9.
Colhoun, E.A., 1980. Glacial diversion of drainage: an example from the cradle mountain national park, northern Tasmania. Aust. Geogr. 14 (6), 365–367. https://doi.org/10.1080/00049188008702785.
Colhoun, E.A., 1996. Application of Iversen's glacial–inter- glacial cycle to interpretation of the last glacial and Holocene vegetation of western Tasmania. Quat. Sci. Rev. 15, 557–580.
Colhoun, E.A., van de Geer, G., 1986. Holocene to middle last glaciation vegetation

history at tullabardine dam, western Tasmania. Proc. R. Soc. B 229, 177–207.
Colhoun, E.A., Pola, J.S., Barton, C.E., Heijnis, H., 1999. Late pleistocene vegetation and climate history of lake selina, western Tasmania. Quat. Int. 57–58, 5–23.
Cosgrove, R., 1995. Late pleistocene behavioural variation and time trends: the case from Tasmania. Archaeol. Ocean. 30, 83–104. https://doi.org/10.1002/j.1834-4453.1995.tb00333.x.
Cosgrove, R., 1999. Forty-two degrees south: the archaeology of late pleistocene Tasmania. J. World Prehistory 13, 357–402. https://doi.org/10.1023/A:1022310029016.
Cosgrove, R., Allen, J., Marshall, B., 1990. Palaeo-ecology and Pleistocene human occupation in south central Tasmania. Antiquity 64, 59–78.
Dodson, J.R., 2001. A vegetation and fire history in a subalpine woodland and rainforest region, Solomons Jewel Lake, Tasmania. Holocene 11, 111–116.
Donders, T.H., Haberle, S.G., Hope, G., Wagner, F., Visscher, H., 2007. Pollen evidence for the transition of the Eastern Australian climate system from the post-glacial to the present-day ENSO mode. Quat. Sci. Rev. 26, 1621–1637. https://doi.org/10.1016/j.quascirev.2006.11.018.
Ellis, R.C., 1985. The relationships among eucalypt forest, grassland and rainforest in a highland area in northeastern Tasmania. Aust. J. Ecol. 10, 297–314.
Fletcher, M.-S., Moreno, P.I., 2011. Zonally symmetric changes in the strength and position of the Southern Westerlies drove atmospheric CO2 variations over the past 14 k.y. Geology 39, 419–422. https://doi.org/10.1130/G31807.1.
Fletcher, M.-S., Moreno, P.I., 2012. Have the Southern Westerlies changed in a zonally symmetric manner over the last 14,000 years? A hemisphere-wide take on a controversial problem. Quat. Int. 253, 32–46. https://doi.org/10.1016/j.quaint.2011.04.042.
Fletcher, M.-S., Thomas, I., 2007a. Holocene vegetation and climate change from near Lake Pedder, south-west Tasmania, Australia. J. Biogeogr. 34, 665–677.
Fletcher, M.-S., Thomas, I., 2007b. Modern pollen-vegetation relationships in western Tasmania, Australia. Rev. Palaeobot. Palynology 146, 146–168. https://doi.org/10.1016/j.revpalbo.2007.03.002.
Fletcher, M.-S., Thomas, I., 2010a. The origin and temporal development of an ancient cultural landscape. J. Biogeogr. 37, 2183–2196. https://doi.org/10.1111/j.1365-2699.2010.02363.x.
Fletcher, M.-S., Thomas, I., 2010b. A quantitative Late Quaternary temperature reconstruction from western Tasmania, Australia. Quat. Sci. Rev. 29, 2351–2361.
Fletcher, M-S., Benson, A., Bowman, D.M.J.S., Heijnis, H., Hopf, F., Mariani, M., Stahle, L.N., Whitlock, C., Zawadzki, A. in review. Long-term rain forest dynamics within a topographic fire refugia. Global Ecology and Biogeography.
Fletcher, M.-S., Wolfe, B.B., Whitlock, C., Pompeani, D.P., Heijnis, H., Haberle, S.G., et al., 2014a. The legacy of mid-Holocene fire on a Tasmanian montane landscape. J. Biogeogr. 41, 476–488. https://doi.org/10.1111/jbi. 12229.
Fletcher, M.-S., Wood, S.W., Haberle, S.G., 2014b. A fire-driven shift from forest to non-forest: evidence for alternative stable states? Ecology 95, 2504–2513. https://doi.org/10.1890/12-1766.1.
Fletcher, M.-S., Benson, A., Heijnis, H., Gadd, P.S., Cwynar, L.C., Rees, A.B.H., 2015. Changes in biomass burning mark the onset of an ENSO-influenced climate regime at 42°S in southwest Tasmania, Australia. Quat. Sci. Rev. 122, 222–232. https://doi.org/10.1016/j.quascirev.2015.05.002.
Gammage, B., 2008. Plain facts: Tasmania under aboriginal management. Landsc. Res. 33, 241–254. https://doi.org/10.1080/01426390701767278.
Gammage, B., 2011. The Biggest Estate on Earth: How Aborigines Made Australia. Allen and Unwin, Sydney, FC.
Gavin, D.G., Oswald, W.W., Wahl, E.R., Williams, J.W., 2003. A statistical approach to evaluating distance metrics and analog assignments for pollen records. Quat. Res. 60, 356–367. https://doi.org/10.1016/S0033-5894(03)00088-7.
Gedye, S.J., Jones, R.T., Tinner, W., Ammann, B., Oldfield, F., 2000. The use of mineral magnetism in the reconstruction of fire history: a case study from Lago di Origlio. Swiss alps. Palaeogeogr. Palaeoclimatol. Palaeoecol. 164, 101–110. https://doi.org/10.1016/S0031-0182(00)00178-4.
Giesecke, T., Ammann, B., Brande, A., 2014. Palynological richness and evenness: insights from the taxa accumulation curve. Veg. Hist. Archaeobotany 23, 217–228.
Gott, B., 2002. Absence of evidence is not evidence of absence. Curr. Anthropol. 43, 650–656.
Gott, B., 2005. Aboriginal fire management in south- eastern Australia: aims and frequency. J. Biogeogr. 32, 1203–1208.
Grimm, E.C., 1988. Data analysis and display. In: Huntley, B., Webb III, T. (Eds.), Vegetation History. Kluwer Academic, Dordrecht, pp. 43–76.
Grimm, E.C., 1990. TILIA and TILIA. GRAPH: PC spreadsheet and graphics software for pollen data (Version 2.0.b.4). INQUA – commission for the study of the Holocene, working-group on data-handling methods. Newsletter 4, 5–7.
Grootes, P.M., Steig, E.J., Stuiver, M., Waddington, E.D., Morse, D.L., 2001. The Taylor Dome Antarctic 18O record and globally synchronous changes in Climate. Quat. Res. 56, 289–298. https://doi.org/10.1006/qres.200 1.2276.
Haberle, S.G., 2005. A 23,000-yr pollen record from Lake euramoo, wet tropics of NE queensland, Australia. Quat. Res. 64, 343–356. https://doi.org/10.1016/j.yqres.2005.08.013.
Harris, S., Kitchener, A., 2005. From forest to fjaeldmark: descriptions of Tasmania's vegetation. In: Department of Primary Industries. Water and Environment, Hobart.
Hendon, H.H., Thompson, D.W.J., Wheeler, M.C., 2007. Australian rainfall and surface temperature variations associated with the southern hemisphere annular mode. J. Clim. 20, 2452–2467. https://doi.org/10.1175/JCLI4134.1.
Higuera, P.E., Brubaker, L.B., Anderson, P.M., Hu, F.S., Brown, T.A., 2009. Vegetation mediated the impacts of postglacial climate change on fire regimes in the southcentral Brooks Range, Alaska. Ecol. Monogr. 79, 201–219. https://doi.org/10.1890/07-2019.1.
Higuera, P.E., Gavin, D.G., Bartlein, P.J., Hallett, D.J., 2010. Peak detection in sediment–charcoal records: impacts of alternative data analysis methods on fire-history interpretations. Int. J. Wildland Fire 19, 996–1014.
Hill, K.J., Santoso, A., England, M.H., 2009. Interannual Tasmanian rainfall variability associated with large-scale climate modes. J. Clim. 22, 4383–4397. https://doi.org/10.1175/2009JCLI2769.1.
Hill, R.S., Jordan, G.J., Macphail, M.K., 2015. Why we should retain *Nothofagus sensu lato*. Aust. Syst. Bot. 28, 190–193. https://doi.org/10.1071/SB15026.
Hogg, A.G., Hua, Q., Blackwell, P.G., Niu, M., Buck, C.E., Guilderson, T.P., et al., 2013. SHCal13 southern hemisphere calibration, 0-50,000 cal BP. Radiocarbon 55, 1889–1903. https://doi.org/10.2458/azu_js_rc.55.16783.
Holz, A.S., Wood, S.W., Veblen, T.T., Bowman, D.M.J.S., 2015. Effects of high-severity fire drove the population collapse of the subalpine Tasmanian endemic conifer Athrotaxis cupressoides. Glob. Change Biol. 21, 445–458. https://doi.org/10.1111/gcb.12674.
Hope, G., 1999. Vegetation and fire response to late Holocene human occupation in island and mainland northwest Tasmania. Quat. Int. 59, 47–60.
Hopf, F.V.L., Colhoun, E.A., Barton, C.E., 2000. Late-glacial and Holocene record of vegetation and climate from cynthia bay, Lake St Clair, Tasmania. J. Quat. Sci. 15, 725–732. https://doi.org/10.1002/1099-1417(200010)15:7<725::AID-JQS563>3.0.CO;2–8.
Hopf, F.V.L., Pearson, S., Shimeld, P., 2005. The Newcastle Pollen Collection, Version 3.03. The University of Newcastle, Australia. http://www.aqua.org.au/AQUA/Pollen/index.html.
Iglesias, V., Whitlock, C., 2014. Fire responses to postglacial climate change and human impact in northern Patagonia (41–43°S). Proc. Natl. Acad. Sci. U. S. A. 101, E5545–E5554. https://doi.org/10.1073/pnas.1410443111.
Jackson, W.D., 1968. Fire and the Tasmanian Flora. Tasmanian Year Book No. 2, Hobart.
Jackson, W.D., 1999. The Tasmanian legacy of man and fire. Pap. Proc. R. Soc. Tasman. 133, 1–14.
Jones, R., 1969. Fire-stick farming. Aust. Nat. Hist. 16, 224–228.
Jones, R., 1995. Establishing the sequences. Annu. Rev. Anthropol. 24, 423–446.
Kelly, R.F., Higuera, P.E., Barrett, C.M., Hu, F.S., 2011. A signal-to-noise index to quantify the potential for peak detection in sediment-charcoal records. Quat. Res. 75, 11–17. https://doi.org/10.1016/j.yqres.2010.07.011.
Kershaw, A.P., Bretherton, S.C., van der Kaars, S., 2007. A complete pollen record of the last 230 ka from Lynch's Crater, north-eastern Australia. Palaeogeogr. Palaeoclimatol. Palaeoecol. 251, 23–45.
Kirkpatrick, J.B., Balmer, J., 1991. The vegetation and higher plant flora of the Cradle Mountain-Pencil Pine area, northern Tasmania. In: Banks, M.R., Smith, S.J., Orchard, A.E., Kantvilas, G. (Eds.), Aspects of Tasmanian Botany: a Tribute to Winifred Curtis. The Royal Society of Tasmania, Hobart, pp. 119–148.
Kirkpatrick, J.B., Bridle, K.L., 2013. Natural and cultural histories of fire differ between Tasmanian and mainland Australian alpine vegetation. Aust. J. Bot. 61, 465–474. https://doi.org/10.1071/BT13128.
Lourandos, H., 1983. 10,000 years in the Tasmanian highlands. Aust. Archaeol. 16, 39–47.
Mackenzie, L., Moss, P., 2014. A Late Quaternary Record of Vegetation and Climate Change from Hazards Lagoon. Quaternary International, eastern Tasmania.
Mackintosh, A.N., Barrows, T.T., Colhoun, E.A., Fifield, L.K., 2006. Exposure dating and glacial reconstruction at Mt. Field, Tasmania, Australia, identifies MIS 3 and MIS 2 glacial advances and climatic variability. J. Quat. Sci. 21, 363–376. https://doi.org/10.1002/jqs.989.
Macphail, M.K., 1975. Late pleistocene environments in Tasmania. Search 6, 295–300.
Macphail, M.K., 1979. Vegetation and climates in southern Tasmania since the last glaciation. Quat. Res. 11, 306–341. https://doi.org/10.1016/0033-5894(79)90078-4.
Mariani, M., Connor, S.E., Fletcher, M.S., Theuerkauf, M., Kunes, P., Jacobsen, G., Saunders, K.M., Zawadzki, A., 2017. How old is the Tasmanian cultural landscape? A test of landscape openness using quantitative land-cover reconstructions. J. Biogeogr. 1–11. https://doi.org/10.1111/jbi.13040.
Markgraf, V., Bradbury, J.P., Busby, J.R., 1986. Paleoclimates in southwestern Tasmania during the last 13,000 years. PALAIOS 1, 368–380. https://doi.org/10.2307/3514474.
Marsden-Smedley, J.B., Kirkpatrick, J.B., 2000. Fire management in Tasmania's Wilderness World Heritage Area: ecosystem restoration using indigenous-style fire regimes? Ecol. Manag. Restor. 1, 195–203.
Marx, S.K., McGowan, H.A., Kamber, B.S., 2009. Long-range dust transport from eastern Australia: a proxy for Holocene aridity and ENSO-type climate variability. Earth Planet. Sci. Lett. 282, 167–177. https://doi.org/10.1016/j.epsl. 2009. 03.013.
McGlone, M., Kershaw, A.P., Markgraf, V., 1992. El nino-southern oscillation and climatic variability in australasian and south american palaeoenvironmental records. In: Diaz, H.F., Markgraf, V. (Eds.), El Nino: Historical and Palaeoclimatic Aspects of the Southern Oscillation. Cambridge University Press, pp. 435–462.
McIntosh, P.D., Price, D.M., Eberhard, R., Slee, A.J., 2009. Late Quaternary erosion events in lowland and mid-altitude Tasmania in relation to climate change and first human arrival. Quat. Sci. Rev. 28, 850–872. https://doi.org/10.1016/j.quascirev.20 08.12.0 03.
McWethy, D.B., Haberle, S.G., Hopf, F., Bowman, D.M.J.S., 2016. Aboriginal impacts

on fire and vegetation on a Tasmanian island. J. Biogeogr. https://doi.org/10.1111/jbi.12935.

Members, E.P.I.C.A., 2004. Eight glacial cycles from an Antarctic ice core. Nature 429, 623–628. https://doi.org/10.1038/nature02599.

Moy, C.M., Seltzer, G.O., Rodbell, D.T., Anderson, D.M., 2002. Variability of El ninao/southern oscillation activity at millennial timescales during the Holocene epoch. Nature 420, 162–165. https://doi.org/10.1038/nature 01194.

Nicholls, N., Lucas, C., 2007. Interannual variation of area burnt in Tasmanian bushfires: relationships with climate and predictability. Int. J. Wildland Fire 16, 540–546. https://doi.org/10.1071/WF06125.

Oksanen, J., Blanchet, F.G., Kindt, R., Legendre, P., Minchin, P.R., O'Hara, R.B., Simpson, G.L., Solymos, P., Henry, M., Stevens, H., vegan, Wagner H., 2015. Community Ecology Package. R Package Version 2.3-2. http://CRAN.R-project.org/package=vegan.

Onfray, R., 2012. Cultural artefacts or 'neglected old parks': the colonisation of rainforests in north-western Tasmania. In: Stubbs, B.J. (Ed.), Chapter 7: Australia's Ever-changing Forests, VI: Proceedings of the Eighth National Conference on Australian Forest History, ISBN 978-0-9757906-2-5.

Pike-Tay, A., Cosgrove, Rss., Garvey, J., 2008. Systematic seasonal land use by late Pleistocene Tasmanian Aborigines. J. Archaeol. Sci. 35, 2532–2544.

Pyrke, A.F., Marsden-Smedley, J.B., 2005. Fire-attributes categories, fire sensitivity, and flammability of Tasmanian vegetation communities. Tasforests 16, 35–46.

R Core Team, 2015. R: a language and environment for statistical computing. R Foundation for Statistical Computing, Vienna. Available online at: https://www.R-project.org/.

Rees, A.B.H., Cwynar, L.C., 2010. Evidence for early postglacial warming in Mount Field national park, Tasmania. Quat. Sci. Rev. 29, 443–454. https://doi.org/10.1016/j.quascirev.2009.10.003.

Rees, A.B.H., Cwynar, L.C., Fletcher, M.-S., 2015. Southern westerly Winds submit to the ENSO regime: a multiproxy paleohydrology record from Lake dobson, Tasmania. Quat. Sci. Rev. 126, 254–263. https://doi.org/10.1016/j.quascirev.2015.08.022.

Risbey, J.S., Pook, M.J., McIntosh, P.C., Wheeler, M.C., Hendon, H.H., 2009. On the remote drivers of rainfall variability in Australia. Mon. Weather Rev. 137, 3233–3253. https://doi.org/10.1175/2009MWR 2861.1.

Rodionov, S.N., 2004. A sequential algorithm for testing climate regime shifts. Geophys. Res. Lett. 31, L09204. https://doi.org/10.1029/2004GL019448.

Romanin, L.M., Hopf, F., Haberle, S.G., Bowman, D.M.J.S., 2016. Fire regime and vegetation change in the transition from Aboriginal to European land management in a Tasmanian eucalypt savanna. Aust. J. Bot. 64, 427–440. https://doi.org/10.1071/BT16032.

Shulmeister, J., Lees, B.G., 1995. Pollen evidence from tropical Australia for the onset of an ENSO-dominated climate at c. 4000 BP. Holocene 5, 10–18.

Sikes, E.L., Howard, W.R., Samson, C.R., Mahan, T.S., Robertson, L.G., Volkman, J.K., 2009. Southern ocean seasonal temperature and subtropical front movement on the South tasman rise in the late quaternary. Paleoceanography 24, 2201. https://doi.org/10.1029/2008PA 001659.

Simpson, G.L., 2007. Analogue methods in palaeoecology: using the analogue package. J. Stat. Softw. 22, 1–29.

Simpson, G.L., Oksanen, J., 2015. Analogue: Analogue Matching and Modern Analogue Technique Transfer Function Models. (R Package Version 0.16-3). http://cran.r-project.org/package=analogue.

Stahle, L.N., Whitlock, C., Haberle, S.G., 2016. A 17,000-year-long record of vegetation and fire from cradle mountain national park, Tasmania. Front. Ecol. Evol. 4, 1–17. https://doi.org/10.3389/fevo.2016.00082.

Stern, N., Marshall, B., 1993. Excavations at Mackintosh 90/1 in western Tasmania: a discussion of stratigraphy chronology and site formation. Archaeol. Ocean. 28, 8–17. https://doi.org/10.1002/j.1834-4453.1993.tb00310.x.

Tepley, A.J., Veblen, T.T., Perry, G.L.W., Stewart, G.H., Naficy, C.E., 2016. Positive feedbacks to fire-driven deforestation following human colonization of the South island of New Zealand. Ecosystems 19, 1325–1344. https://doi.org/10.1007/s10021-016-0008-9.

Thomas, I., 1991. The Holocene archaeology and palaeoecology of northeastern Tasmania, Australia. Ph.D. thesis. In: Department of Geography and Environmental Studies. University of Tasmania, Hobart.

Thomas, I., 1993. Late Pleistocene environments and aboriginal settlement patterns in Tasmania. Aust. Archaeol. 36, 1–11.

Thrush, M.N., 2008. The Pleistocene Glaciations of the Cradle Mountain Region, Tasmania. Ph.D. thesis. University of Newcastle, New South Wales.

Trauernicht, C., Brook, B.W., Murphy, B.P., Williamson, G.J., Bowman, D.M.J.S., 2015. Local and global pyrogeographic evidence that indigenous fire management creates pyrodiversity. Ecol. Evol. 5, 1908–1918.

Wanner, H., Beer, J., Bütikofer, J., Crowley, T.J., Cubasch, U., Flückiger, J., et al., 2008. Mid- to Late Holocene climate change: an overview. Quat. Sci. Rev. 27, 1791–1828. https://doi.org/10.1016/j.quascirev.2008.06.013.

Wells, P., Hickey, J., 2005. Wet sclerophyll, mixed and swamp forest. In: Reid, J.B., Hill, R.S., Brown, M.J., Hovenden, M.J. (Eds.), Vegetation of Tasmania, Flora of Australia Supplementary Series No. 8. Australian Biological Research Study, Tasmania.

Whitlock, C., Larsen, C.P.S., 2001. Charcoal as a fire proxy. In: Smol, J.P., Birks, H.J.P., Last, W.M. (Eds.), Tracking Environmental Change Using Lake Sediments, vol. 3. Kluwer Academic Publishers, Dordrecht, pp. 75–97. Terrestrial, Algal, and Siliceous Indicators.

Whitlock, C., Moreno, P.I., Bartlein, P., 2007. Climatic controls of Holocene fire patterns in southern South America. Quat. Res. 68, 28–36. https://doi.org/10.1016/j.yqres.2007.01.012.

Wilkins, D., Gouramanis, C., De Deckker, P., Fifield, L.K., Olley, J., 2013. Holocene lake-level fluctuations in lakes Keilambete and Gnotuk, southwestern Victoria, Australia. Holocene 23, 784–795. https://doi.org/10.1177/0959683612471983.

Williamson, G.J., Prior, L.D., Jolly, W.M., Cochrane, M.A., Murphy, B.P., Bowman, D.M.J.S., 2016. Measurement of inter- and intra-annual variability of landscape fire activity at a continental scale: the Australian case. Environ. Res. Lett. 11, 035003. https://doi.org/10.1088/1748-9326/11/3/035003.

Wood, S.W., Murphy, B.P., Bowman, D.M.J.S., 2011. Firescape ecology: how topography determines the contrasting distribution of fire and rain forest in the south-west of the Tasmanian Wilderness World Heritage Area. J. Biogeogr. 38, 1807–1820. https://doi.org/10.1111/j.1365-2699.2011.0 2524.x.

Xia, Q.K., Zhao, J.-X., Collerson, K.D., 2001. Early-mid Holocene climatic variations in Tasmania, Australia: multi-proxy records in a stalagmite from Lynds Cave. Earth Planet. Sci. Lett. 194, 177–187. https://doi.org/10.1016/S0012-821X(01)00541-6.

Yospin, G.I., Wood, S.W., Holz, A., Bowman, D.M.J.S., Keane, R.E., Whitlock, C., 2015. Modeling vegetation mosaics in sub-alpine Tasmania under various fire regimes. Model. Earth Syst. Environ. 1, 16. https://doi.org/10.1007/s40808-015-0019-0.

Zhao, J.-X., Xia, Q.K., Collerson, K.D., 2001. Timing and duration of the Last Interglacial inferred from high resolution U-series chronology of stalagmite growth in Southern Hemisphere. Earth Planet. Sci. Lett. 184, 633–644. https://doi.org/10.1016/S0012-821X(00)00353-8.